

Functional Renormalization Group Study of the Chiral Phase Transition Including Vector and Axial-vector Mesons

Jürgen Eser

eser@th.physik.uni-frankfurt.de

Mara Grahl

grahl@th.physik.uni-frankfurt.de

Dirk H. Rischke

drischke@th.physik.uni-frankfurt.de

Johann Wolfgang Goethe-Universität

Max-von-Laue-Str. 1, D-60438 Frankfurt am Main, Germany

October 8, 2018

Abstract

The transition in quantum chromodynamics (QCD) from hadronic matter to the quark-gluon plasma (QGP) at high temperatures and/or net-baryon densities is associated with the restoration of chiral symmetry and can be investigated in the laboratory via heavy-ion collisions. We study this chiral transition within the functional renormalization group (FRG) approach applied to the two-flavor version of the extended Linear Sigma Model (eLSM). The eLSM is an effective model for the strong interaction and features besides scalar and pseudoscalar degrees of freedom also vector and axial-vector mesons. We discuss the impact of the quark masses and the axial anomaly on the order of the chiral transition. We also confirm the degeneracy of the masses of chiral partners above the transition temperature. We find that the mass of the a_1 meson (ρ meson) decreases (increases) towards the chiral transition.

1 Introduction

QCD is the fundamental theory of the strong interaction. For massless quarks, the QCD Lagrangian has a global $U(N_f)_R \times U(N_f)_L \cong SU(N_f)_V \times SU(N_f)_A \times U(1)_V \times U(1)_A$ symmetry, where N_f denotes the number of quark flavors. The $U(1)_V$ symmetry corresponds to baryon-number conservation, which is always respected. At the quantum level, $U(1)_A$ is broken to $\mathbb{Z}(N_f)_A$, a phenomenon which is referred to as the axial anomaly [1]. In the QCD vacuum, the remaining $SU(N_f)_V \times SU(N_f)_A$ symmetry, termed “chiral symmetry” in the following, is further spontaneously broken to $SU(N_f)_V$ by a non-vanishing quark condensate $\langle \bar{q}q \rangle$, inducing $N_f^2 - 1$ Goldstone bosons [2, 3, 4]. For nonzero and degenerate quark masses, the chiral symmetry is also explicitly broken to $SU(N_f)_V$.

At high temperatures and/or net-baryon number densities, the quark condensate melts and chiral symmetry is effectively restored. This chiral transition is commonly associated with the so-called QCD transition between a hadronic phase and the QGP. The QGP state has existed during the early stages of the universe. Experiments at accelerator facilities, such as SPS and LHC at CERN, RHIC at BNL, or SIS-100/300 at the FAIR project in Darmstadt, aim to explore the QGP via heavy-ion collisions [5]. Above the chiral transition, the masses of chiral partners, such as the sigma and the pion or the ρ and the a_1 meson, become degenerate [6]. In particular, dropping ρ and a_1 meson masses were suggested as signatures for chiral symmetry restoration [7, 8, 9]. The change of the spectral properties of the ρ meson

during the chiral transition could, e.g., be detected via its decay into dileptons [10]. Modifications of the dilepton spectrum have been observed in Pb+Pb [11] and In+In [12] collisions. Concerning the axial anomaly, it was claimed in Ref. [13] that data for Au+Au collisions at RHIC energies show a reduction of the η' meson mass, which was interpreted as a precursor for an effective restoration of the $U(1)_A$ symmetry [14].

In general, the order of the chiral transition depends on the number N_f of quark flavors and their masses [15]. Furthermore, for $N_f = 2$, the order depends on whether the $U(1)_A$ symmetry is restored prior to the restoration of chiral symmetry [16], or whether it remains broken by the axial anomaly. For vanishing quark masses, Pisarski and Wilczek [17] have argued that, in the absence of the $U(1)_A$ anomaly, the chiral phase transition for $N_f \geq 2$ is of first order and, in the presence of the $U(1)_A$ anomaly, can be of second order for $N_f = 2$. For an infinite anomaly strength and if the transition is of second order, it definitely falls into the $O(4)$ -universality class [as originally conjectured by the authors of Ref. [17]]. Recently, however, it was argued that the chiral transition can be of second order for $N_f = 2$, no matter whether the axial anomaly is present [18] or not [19, 20], only the associated universality class differs: it was conjectured that the second-order transition can be in the $SU(2)_A \times U(2)_V$ class for finite anomaly strength, and in the $U(2)_A \times U(2)_V$ class for zero anomaly strength, respectively. For nonzero quark masses, the second-order transition is smeared out into a crossover.

The chiral transition has been extensively investigated from first principles via lattice QCD [21, 22, 23, 24, 25, 26, 27, 28, 29]. The critical temperature for vanishing quark-chemical potential, $\mu = 0$, was estimated to be ≈ 160 MeV [29, 30, 31, 32, 33]. Lattice-QCD calculations do not agree upon whether the $U(1)_A$ symmetry has already been restored at the chiral transition temperature [34, 35] or not [36, 37, 38]. Unfortunately, perturbative methods fail to achieve reliable results in the low-energy range, where the gauge coupling is strong. Besides, they are plagued by severe infrared divergences. Therefore, non-perturbative continuum methods, such as the functional renormalization group (FRG) [39, 40, 41, 42], are complementary to lattice QCD and hence indispensable for exploring the nature of QCD matter.

FRG studies of the chiral transition using effective models for QCD have a long tradition [43]: a quark-meson model with $U(2)_R \times U(2)_L$ symmetry has been investigated beyond the local potential approximation (LPA) in Ref. [44, 45]. An $O(N)$ -symmetric quark-meson model was studied in Ref. [46]. The phase structures of the chiral quark-meson model and the Polyakov-quark-meson(-diquark) model for the two lightest flavors as well as for 2+1 flavors were determined in Refs. [47, 48, 49, 50, 51, 52, 53, 54, 55, 56, 57]. $U(1)_A$ -violating terms in the FRG were introduced in Ref. [58]. For massless up and down quarks and a physical strange quark, the chiral transition was shown to be of first/second order without/with the $U(1)_A$ anomaly in the framework of a quark-meson model [59, 60]. Also non-vanishing external magnetic fields were studied in such a model [61, 62]. Recent insights into second-order and fluctuation-induced first-order phase transitions in a $U(2)_R \times U(2)_L$ symmetric model with scalar and pseudoscalar mesons were provided e.g. in Refs. [63, 64]. The influence of the $U(1)_A$ anomaly in a purely mesonic model was studied in Ref. [18]. The infrared-stable $U(2)_V \times U(2)_A$ fixed point detected in Ref. [19] was also found with the help of the FRG technique, but the subsequent stability analysis remained inconclusive [20]. FRG studies based on QCD degrees of freedom were presented in Refs. [41, 65, 66, 67, 68, 69].

Vector-meson fields were introduced into a chiral effective nucleon-meson Lagrangian in Refs. [70, 71, 72, 73, 74] and the phase diagram at nonvanishing net-baryon density was studied within the FRG. However, the vector-meson degrees of freedom were only considered to be background fields, i.e., their fluctuations were neglected in the FRG flow. A first FRG study of (axial-)vector mesons in QCD at $T = \mu = 0$ was performed in Ref. [75], revealing that the hadronic contributions to the flow in vacuum are dominated by the sigma meson and the pions.

A study of the chiral transition at nonzero temperature within the FRG including vector and axial-vector mesons is, however, still missing. In this work, we fill this gap by applying the FRG to a purely mesonic model. We ascertain the mass degeneracy of chiral partners above the transition and identify its order. We consider the so-called eLSM [76, 77, 78] as effective model for the strong interaction at nonzero T and for vanishing μ . This model has been shown to reproduce hadronic vacuum properties such as masses and decay widths to a surprising degree of accuracy [78]. Furthermore, it has the same low-energy limit as QCD [79]. We study this model in a limit where it resembles the time-honored Sakurai model [80, 81].

This paper is organized as follows: in Sec. 2.1 we introduce the two-flavor version of the eLSM. The subsequent part (Sec. 2.2) discusses the FRG formalism to describe fluctuations of spin-zero and spin-

one mesons. The numerical results for vanishing quark masses in the absence (or presence) of the axial anomaly are presented in Sec. 3.1 (3.2). The case of explicit breaking of chiral symmetry by nonzero quark masses is discussed in Sec. 3.3. Section 4 concludes this work with a summary of our results and an outlook.

We use natural units $\hbar = c = k_B = 1$ and work in a finite $(3 + 1)$ -dimensional Euclidean spacetime volume $V \times (0, 1/T]$ at nonzero temperature T with periodic boundary conditions and, consequently, a discrete momentum spectrum: $q = (\omega_n, \vec{q})$, where the Matsubara frequencies for bosonic fields are given by $\omega_n = 2n\pi T$. We use a shorthand notation for spacetime integrations:

$$\int_{\mathcal{V}} d^{3+1}x = \int_0^{1/T} d\tau \int_V d^3x = \int_x, \quad (1)$$

with $\mathcal{V} = V/T$. We employ Einstein's summation convention, i.e., indices appearing twice are summed over. If these indices are Lorentz indices, $\mu = 0, 1, 2, 3$, it does not matter whether they appear as co- or contravariant indices, because we work in Euclidean spacetime. We shall always use covariant Lorentz indices.

2 Methods

2.1 Extended Linear Sigma Model

At low energies, quarks and gluons are confined inside hadrons, which are thus the effective degrees of freedom. An effective theory for hadrons must incorporate the chiral symmetry of QCD, as well as its spontaneous breaking. We work with a mesonic linear sigma model [82, 83] as an effective implementation of the strong interaction, which, besides scalar and pseudoscalar mesons, also includes vector and axial-vector mesons [6, 76, 84, 85, 86]: the so-called eLSM [77]. The scalar and pseudoscalar fields are the real and imaginary parts of a complex $N_f \times N_f$ matrix Σ that lives in the $[N_f^*, N_f]$ representation of the group $U(N_f)_R \times U(N_f)_L$. Under transformations of this group, Σ behaves as follows:

$$\Sigma \rightarrow U_R^\dagger \Sigma U_L, \quad (2)$$

where the group elements $U_{R,L}$ are unitary matrices. In terms of hadronic fields, $\Sigma = (\sigma_a + i\pi_a)t_a$, with the generators t_a of $U(2)$ in the fundamental representation ($\text{tr}[t_a t_b] = \delta_{ab}/2$). Here, σ_a and π_a represent scalar and pseudoscalar degrees of freedom, respectively. Analogously, we define right- and left-handed fields for (axial-)vector mesons (parametrized by axial-vector fields $A_{a,\mu}$ and vector fields $V_{a,\mu}$): $R_\mu = (V_{a,\mu} + A_{a,\mu})t_a$, $L_\mu = (V_{a,\mu} - A_{a,\mu})t_a$. They transform as:

$$R_\mu \rightarrow U_R^\dagger R_\mu U_R, \quad L_\mu \rightarrow U_L^\dagger L_\mu U_L. \quad (3)$$

The globally chirally symmetric Lagrangian is given by [77]:

$$\begin{aligned} \mathcal{L} = & \text{tr} \left[(D_\mu \Sigma)^\dagger D_\mu \Sigma \right] + m_0^2 \text{tr} (\Sigma^\dagger \Sigma) + \lambda_1 [\text{tr} (\Sigma^\dagger \Sigma)]^2 + \lambda_2 \text{tr} \left[(\Sigma^\dagger \Sigma)^2 \right] + \frac{1}{4} \text{tr} (L_{\mu\nu}^2 + R_{\mu\nu}^2) \\ & + \text{tr} \left[\left(\frac{m_1^2}{2} + \Delta \right) (L_\mu^2 + R_\mu^2) \right] - \text{tr} [H (\Sigma + \Sigma^\dagger)] - c_A (\det \Sigma + \det \Sigma^\dagger) \\ & - i g_2 (\text{tr} \{ L_{\mu\nu} [L_\mu, L_\nu] \} + \text{tr} \{ R_{\mu\nu} [R_\mu, R_\nu] \}) + \frac{h_1}{2} \text{tr} (\Sigma^\dagger \Sigma) \text{tr} (L_\mu^2 + R_\mu^2) \\ & + h_2 \text{tr} \left(|R_\mu \Sigma|^2 + |\Sigma L_\mu|^2 \right) + 2h_3 \text{tr} (\Sigma L_\mu \Sigma^\dagger R_\mu) - g_3 [\text{tr} (L_\mu L_\nu L_\mu L_\nu) + \text{tr} (R_\mu R_\nu R_\mu R_\nu)] \\ & - g_4 [\text{tr} (L_\mu L_\mu L_\nu L_\nu) + \text{tr} (R_\mu R_\mu R_\nu R_\nu)] - g_5 \text{tr} (L_\mu L_\mu) \text{tr} (R_\nu R_\nu) \\ & - g_6 [\text{tr} (L_\mu L_\mu) \text{tr} (L_\nu L_\nu) + \text{tr} (R_\mu R_\mu) \text{tr} (R_\nu R_\nu)], \end{aligned} \quad (4)$$

with the covariant derivative $D_\mu \Sigma = \partial_\mu \Sigma + i g_1 (\Sigma L_\mu - R_\mu \Sigma)$ and the right-/left-handed field-strength tensors $R_{\mu\nu} = \partial_\mu R_\nu - \partial_\nu R_\mu$ and $L_{\mu\nu} = \partial_\mu L_\nu - \partial_\nu L_\mu$. The term $\det \Sigma + \det \Sigma^\dagger$ accounts for the $U(1)_A$ anomaly by breaking $U(N_f)_R \times U(N_f)_L$ to $SU(N_f)_V \times SU(N_f)_A \times U(1)_V$. Its strength is determined by

the coupling constant c_A . The flavor-diagonal terms $\text{tr} [H (\Sigma + \Sigma^\dagger)]$ and $\text{tr} [\Delta (L_\mu^2 + R_\mu^2)]$ correspond to explicit symmetry breaking (ESB) in the (pseudo-)scalar and (axial-)vector sector, respectively:

$$H = \sum_{i=1}^{N_f} h_0^{i^2-1} t_{i^2-1}, \quad \Delta = \text{diag} [\delta_1, \delta_2, \dots, \delta_{N_f}] \propto \text{diag} [m_u^2, m_d^2, \dots, m_{N_f}^2]. \quad (5)$$

For nonzero and degenerate quark masses $m_u^2 = m_d^2 = \dots$ ($h_0^0 \neq 0$, while all other $h_0^{i^2-1}$ vanish; $\Delta \propto \mathbb{1}$ has no further impact), these terms break the $U(N_f)_R \times U(N_f)_L$ symmetry to $U(N_f)_V$.

It should be mentioned that there is a second way of introducing spin-one degrees of freedom to this effective theory. Within the gauged linear sigma model (gLSM) [81, 84], (axial-)vector mesons are treated as massive Yang-Mills fields, accounting for the phenomenon of vector-meson dominance [80, 87]. This model is constructed by requiring local $U(N_f)_R \times U(N_f)_L$ symmetry. The gauge principle calls for a universal coupling of right- and left-handed vector fields to (pseudo-)scalars as well as among spin-one fields themselves. But due to the nonzero mass of the ‘‘gauge bosons’’, of course, the gLSM is not a true gauge theory and the local invariance is already broken down to a global one. Since chiral symmetry is of global nature in QCD anyway, it seems to be logical to work with the Lagrangian (4). Moreover, the ‘‘local’’ version does not reproduce the correct phenomenology of ρ and a_1 mesons [6, 87], a problem which is solved by the globally symmetric eLSM [78].

In this study, we restrict ourselves to the isospin-symmetric two-flavor case, i.e., up and down quarks have the same mass. Hence we are dealing with scalar fields (σ, \vec{a}_0) , pseudoscalars $(\eta, \vec{\pi})$, and with (f_1, \vec{a}_1) as well as $(\omega, \vec{\rho})$ in the (axial-)vector mesonic sector. The fields σ, η, ω , and f_1 are $SU(2)$ -singlet states, whereas the others form isospin triplets. The field η does not correspond to the physical η/η' mesons, which are mixtures of $\bar{n}n$ and $\bar{s}s$ ($n = u, d$ stands for the nonstrange up and down quarks, s for the strange quark). As a first step in applying the FRG to the eLSM, we want to keep things simple and set the constants g_2, g_3, \dots, g_6 as well as h_1, h_2, h_3 to zero. The above defined complex 2×2 - matrices explicitly read:

$$\Sigma = (\sigma + i\eta)t_0 + (\vec{a}_0 + i\vec{\pi}) \cdot \vec{t}, \quad (6)$$

$$R_\mu = (\omega_\mu + f_{1\mu})t_0 + (\vec{\rho}_\mu + \vec{a}_{1\mu}) \cdot \vec{t}, \quad (7)$$

$$L_\mu = (\omega_\mu - f_{1\mu})t_0 + (\vec{\rho}_\mu - \vec{a}_{1\mu}) \cdot \vec{t}, \quad (8)$$

and the different parts of \mathcal{L} can be expressed as:

$$\begin{aligned} \text{tr} [(D_\mu \Sigma)^\dagger D_\mu \Sigma] &= \frac{1}{2} [\partial_\mu \sigma + g_1 (\eta f_{1\mu} + \vec{\pi} \cdot \vec{a}_{1\mu})]^2 + \frac{1}{2} [\partial_\mu \eta - g_1 (\sigma f_{1\mu} + \vec{a}_0 \cdot \vec{a}_{1\mu})]^2 \\ &\quad + \frac{1}{2} [\partial_\mu \vec{a}_0 + g_1 (\vec{\rho}_\mu \times \vec{a}_0 + \eta \vec{a}_{1\mu} + \vec{\pi} f_{1\mu})]^2 \\ &\quad + \frac{1}{2} [\partial_\mu \vec{\pi} - g_1 (\vec{\pi} \times \vec{\rho}_\mu + \sigma \vec{a}_{1\mu} + \vec{a}_0 f_{1\mu})]^2, \end{aligned} \quad (9)$$

$$m_0^2 \text{tr} (\Sigma^\dagger \Sigma) = \frac{m_0^2}{2} (\sigma^2 + \vec{a}_0^2 + \eta^2 + \vec{\pi}^2), \quad (10)$$

$$\lambda_1 [\text{tr} (\Sigma^\dagger \Sigma)]^2 = \frac{\lambda_1}{4} (\sigma^2 + \vec{a}_0^2 + \eta^2 + \vec{\pi}^2)^2, \quad (11)$$

$$\begin{aligned} \lambda_2 \text{tr} [(\Sigma^\dagger \Sigma)^2] &= \frac{\lambda_2}{4} \left\{ \frac{1}{2} (\sigma^2 + \vec{a}_0^2 + \eta^2 + \vec{\pi}^2)^2 \right. \\ &\quad \left. + 2 [(\sigma^2 + \vec{\pi}^2) (\eta^2 + \vec{a}_0^2) - (\sigma\eta - \vec{\pi} \cdot \vec{a}_0)^2] \right\}, \end{aligned} \quad (12)$$

$$\begin{aligned} \frac{1}{4} \text{tr} (L_{\mu\nu}^2 + R_{\mu\nu}^2) &= \frac{1}{4} (\partial_\mu \omega_\nu - \partial_\nu \omega_\mu)^2 + \frac{1}{4} (\partial_\mu \vec{\rho}_\nu - \partial_\nu \vec{\rho}_\mu)^2 \\ &\quad + \frac{1}{4} (\partial_\mu f_{1\nu} - \partial_\nu f_{1\mu})^2 + \frac{1}{4} (\partial_\mu \vec{a}_{1\nu} - \partial_\nu \vec{a}_{1\mu})^2, \end{aligned} \quad (13)$$

$$\frac{m_1^2}{2} \text{tr} (L_\mu^2 + R_\mu^2) = \frac{m_1^2}{2} (f_{1\mu}^2 + \vec{a}_{1\mu}^2 + \omega_\mu^2 + \vec{\rho}_\mu^2), \quad (14)$$

$$\text{tr} [H (\Sigma + \Sigma^\dagger)] = h_0^0 \sigma, \quad (15)$$

$$c_A (\det \Sigma + \det \Sigma^\dagger) = \frac{c_A}{2} (\sigma^2 - \vec{a}_0^2 - \eta^2 + \vec{\pi}^2). \quad (16)$$

Obviously, the ω meson completely decouples from any interactions. This would not be the case had we included other terms from Eq. (4).

In the low-temperature broken phase, the isoscalar σ field acquires a non-vanishing expectation value $\langle\sigma\rangle_0 = \langle\bar{q}q\rangle = \text{const.} \neq 0$ (here, the angular brackets are the notation for expectation values and the subscript 0 denotes the absence of external sources). Therefore, one has to consider fluctuations around the physical ground state and thus a shift of the σ field by its expectation value: $\sigma \rightarrow \langle\sigma\rangle_0 + \sigma$. The expectation value $\langle\sigma\rangle_0$ acts as the order parameter for the chiral phase transition. After accounting for this shift, integration by parts then gives rise to the bilinear terms $g_1 \langle\sigma\rangle_0 \eta \partial_\mu f_{1\mu}$ and $g_1 \langle\sigma\rangle_0 \vec{\pi} \cdot \partial_\mu \vec{a}_{1\mu}$. They represent the so-called π - a_1 - and η - f_1 -mixing, leading to nondiagonal elements in the scattering matrix. Usually these terms are eliminated. Following Ref. [81], this is done by shifting the axial-vector fields: $f_{1\mu} \rightarrow f_{1\mu} + w \partial_\mu \eta$ and $\vec{a}_{1\mu} \rightarrow \vec{a}_{1\mu} + w \partial_\mu \vec{\pi}$ with $w = g_1 \langle\sigma\rangle_0 / [m_1^2 + (g_1 \langle\sigma\rangle_0)^2]$. In turn, the axial-vector fields become explicitly RG-scale dependent (through the dependence of w on $\langle\sigma\rangle_0$) and the pseudoscalar states need to be renormalized: $\pi_a \rightarrow \sqrt{Z_\pi} \pi_a$, $Z_\pi = 1 + (g_1 \langle\sigma\rangle_0)^2 / m_1^2$. This provides the canonical normalization of all one-meson states, such that their Fourier components can be interpreted as creation and annihilation operators in the process of quantization [84]. For a precise discussion of the σ shift and its implications on the FRG flow we refer to Ref. [75]. Instead of redefining the a_1 and f_1 fields, one may also work with nondiagonal propagators as performed in Ref. [87].

The vacuum expectation value $\langle\sigma\rangle_0$ is the minimum of the classical potential energy density $V(\langle\sigma\rangle)$:

$$V(\langle\sigma\rangle) = \frac{1}{2} (m_0^2 - c_A) \langle\sigma\rangle^2 + \frac{1}{4} \left(\lambda_1 + \frac{\lambda_2}{2} \right) \langle\sigma\rangle^4 - h_0^0 \langle\sigma\rangle, \quad \left. \frac{dV}{d\langle\sigma\rangle} \right|_{\langle\sigma\rangle=\langle\sigma\rangle_0} = 0. \quad (17)$$

The wave-function renormalization Z_π is related to $\langle\sigma\rangle_0$ and to the masses of the a_1 and ρ mesons by:

$$\langle\sigma\rangle_0 = \sqrt{Z_\pi} f_\pi \equiv f_\pi \frac{m_{a_1}}{m_\rho}, \quad (18)$$

where $f_\pi \simeq 93$ MeV is the pion decay constant. The KSFR (Kawarabayashi-Suzuki-Fayyazuddin-Riazuddin) relation [88, 89] predicts that $Z_\pi = 2$. This slightly differs from the value of $Z_\pi \simeq (m_{a_1}/m_\rho)^2 \simeq 2.552$ quoted by the particle data group [90].

The identification of the mesonic fields with measured resonances listed in Ref. [90] is partly straightforward: the pions and the η (as the pure $\bar{n}n$ state arising from unmixing the physical η and η') have a mass around 140 MeV and 700 MeV, respectively. The vector fields ω and ρ represent the $\omega(782)$ and $\rho(770)$ resonances. The axial vectors f_1 and a_1 correspond to the $f_1(1285)$ and $a_1(1260)$. For the σ and the a_0 fields, however, it is controversial whether they should describe $\{f_0(500), a_0(980)\}$ or $\{f_0(1370), a_0(1450)\}$. It was argued in Refs. [76, 77, 78] that the latter option might be favored.

2.2 Functional renormalization group

The Wilsonian renormalization group (RG) performs the mode integration of (quantum-)statistical fluctuations from the ultraviolet (UV) to the infrared (IR) in a stepwise manner, i.e., it successively takes momentum-shell by momentum-shell into account [91, 92, 93, 94, 95, 96, 97]. The FRG is an implementation of this procedure which allows us to non-perturbatively formulate quantum field theories in terms of a differential equation. This flow equation dictates the scale (k -) dependence of the effective average action Γ_k , which interpolates between the bare interactions at some UV cutoff scale $k_{\text{UV}} = \Lambda$ and the macroscopic physics including all fluctuations in the IR, $k_{\text{IR}} = 0$. A k -dependent term ΔS_k is added to the action S in order to provide an effective cutoff at momenta $q^2 \simeq k^2$, such that only modes with $q^2 \gtrsim k^2$ are integrated out in the RG flow. The term ΔS_k regulates the scale evolution of Γ_k in such a way that the full effective action $\Gamma \equiv \Gamma_{k \rightarrow 0}$ is obtained in the IR limit. The effective action Γ is the generating functional of one-particle irreducible vertex diagrams of the theory. For $k \rightarrow \Lambda$, in contrast, the classical action is recovered: $\Gamma_{k \rightarrow \Lambda} = S$.

Our investigations focus on the theory defined by the Lagrangian (4). In order to simplify the following discussion, we denote (pseudo-)scalar fields by φ_i and (axial-)vector fields by $A_{i,\mu}$. The field-strength tensors of the latter are denoted as $F_{i,\mu\nu} = \partial_\mu A_{i,\nu} - \partial_\nu A_{i,\mu}$. The fields φ_i and $A_{i,\mu}$ are subject to thermal (for $T > 0$) as well as to quantum fluctuations (also at $T = 0$). Following the discussion in Ref. [98], we

apply Stueckelberg's Lagrangian [99, 100] with coupling λ_{St} to derive the FRG flow equation:

$$S = \int_x \mathcal{L} \rightarrow \int_x \left(\mathcal{L} + \frac{\lambda_{\text{St}}}{2} \partial_\mu A_{i,\mu} \partial_\nu A_{i,\nu} \right). \quad (19)$$

(Axial-)vector mesonic fields usually have three physical degrees of freedom. The additional term in Eq. (19), however, promotes the unphysical fourth to a physical one. Hence, in the following, all vector fields initially have four instead of three degrees of freedom. Although not necessary to ensure renormalizability [75], this formalism guarantees that we work with invertible inverse tree-level propagators [81]. Furthermore, this strategy allows to derive the grand canonical partition function in a simple manner [98].

As a starting point for deriving the FRG flow equation of the theory at hand, we consider the scale-dependent generating functional W_k for connected Green's functions:

$$W_k [J_i, J_{i,\mu}] \equiv \ln Z_k [J_i, J_{i,\mu}] = \ln \int \mathcal{D}\varphi_i \mathcal{D}A_{i,\mu} e^{-S[\varphi_i, A_{i,\mu}] - \Delta S_k[\varphi_i, A_{i,\mu}] + \int_x J_i \varphi_i + \int_x J_{i,\mu} A_{i,\mu}}. \quad (20)$$

As discussed above, we add a regulator term ΔS_k to the action:

$$\Delta S_k [\varphi_i, A_{i,\mu}] = \frac{1}{2} \mathcal{V} \sum_q [\varphi_i(-q) R_k^{\text{S}}(q) \varphi_i(q) + A_{i,\mu}(-q) R_{k,\mu\nu}^{\text{V}}(q) A_{i,\nu}(q)], \quad (21)$$

which can be interpreted as a momentum-dependent mass term, and we also included sources J_i and $J_{i,\mu}$ for scalar and vector fields. To ensure the required UV/IR limits for the flow of Γ_k , the regulator functions $R_k^{\text{S}}(q)$ and $R_{k,\mu\nu}^{\text{V}}(q)$ must fulfill the following relations: $R_k^{\text{S}}(q), R_{k,\mu\nu}^{\text{V}}(q) \rightarrow 0$ for $k \rightarrow 0$, as well as $R_k^{\text{S}}(q), R_{k,\mu\nu}^{\text{V}}(q) \rightarrow \infty$ for $k \rightarrow \Lambda$. On top of that, the regulators should satisfy: $R_k^{\text{S}}(q), R_{k,\mu\nu}^{\text{V}}(q) \sim k^2$ for $q \rightarrow 0$ and $R_k^{\text{S}}(q), R_{k,\mu\nu}^{\text{V}}(q) \sim 0$ for $q \rightarrow \infty$. Apparently, low-energy fluctuations ($q^2 \ll k^2$) are effectively separated from the RG integration process by giving them an additional ‘‘mass’’ $\sim k^2$, while fast modes ($q^2 \gg k^2$) are not influenced. The effective average action $\Gamma_k + \Delta S_k$ is the Legendre transform of W_k , or in other words:

$$\Gamma_k [\phi_{k,i}, \mathcal{A}_{k,i,\mu}] = \mathcal{V} \sum_q [J_i(-q) \phi_{k,i}(q) + J_{i,\mu}(-q) \mathcal{A}_{k,i,\mu}(q)] - W_k [J_i, J_{i,\mu}] - \Delta S_k [\phi_{k,i}, \mathcal{A}_{k,i,\mu}], \quad (22)$$

where $\phi_{k,i}(q) = \langle \varphi_i(q) \rangle \equiv \mathcal{V}^{-1} \delta W_k / \delta J_i(-q)$ and $\mathcal{A}_{k,i,\mu}(q) = \langle A_{i,\mu}(q) \rangle \equiv \mathcal{V}^{-1} \delta W_k / \delta J_{i,\mu}(-q)$ are the expectation values of the fields in the presence of the sources J_i and $J_{i,\mu}$. Although the Legendre transform $\Gamma_k + \Delta S_k$ is convex by definition, this does not hold for Γ_k itself, as ΔS_k is not necessarily curved in the same way. Exclusively in the case $k \rightarrow 0$, where $\Delta S_k \rightarrow 0$, $\Gamma_{k \rightarrow 0} = \Gamma$ becomes the true Legendre transform of $W_{k \rightarrow 0} \equiv W$, and thus is definitely convex.

For fixed values of the fields, differentiation of Eq. (22) with respect to k yields the FRG flow equation:

$$\partial_k \Gamma_k = \frac{1}{2} \mathcal{V} \sum_q \{ \text{tr} [\mathbf{G}_k^{\text{S}}(q, q) \partial_k \mathbf{R}_k^{\text{S}}(q)] + \text{tr} [\mathbf{G}_{k,\mu\nu}^{\text{V}}(q, q) \partial_k \mathbf{R}_{k,\nu\mu}^{\text{V}}(q)] \}. \quad (23)$$

Here, \mathbf{G}_k^{S} and $\mathbf{G}_{k,\mu\nu}^{\text{V}}$ denote the full propagators for scalar and vector fields. Introducing the general field notation $\Phi = (\phi_{k,i}, \mathcal{A}_{k,i,\mu})$ and using the fact that $\mathcal{V} \mathbf{G}_k = \left(\mathbf{\Gamma}_k^{(2)} + \mathbf{R}_k \right)^{-1}$, Eq. (23) simplifies to:

$$\partial_k \Gamma_k = \frac{1}{2} \text{tr} \left[\left(\mathbf{\Gamma}_k^{(2)} + \mathbf{R}_k \right)^{-1} \partial_k \mathbf{R}_k \right]. \quad (24)$$

The momentum summation has been included in the definition of the trace. The propagators \mathbf{G}_k and \mathbf{R}_k are matrix-valued in momentum space and in all internal spaces.

In principle, the FRG equation and the resulting macroscopic physical observables should be independent of the form of the regulators, which are only restricted by the limits discussed above. In this case, all trajectories in coupling space predicted by different choices of \mathbf{R}_k start at the point $\Gamma_{k \rightarrow \Lambda} = S$ and terminate at $\Gamma_{k \rightarrow 0} = \Gamma$. In practice, however, one needs to truncate the infinite hierarchy of flow equations

arising from Eq. (24) in order to solve them. Indeed, this fact inevitably leads to a regulator-dependent bias, which, fortunately, can be minimized by working with the optimized Litim regulator [101].

One convenient truncation scheme is the expansion of Γ_k in terms of field derivatives [42, 43]. For a purely scalar theory, this would read:

$$\Gamma_k[\Phi] = \int_x \left[U_k(\Phi) + \frac{1}{2} \mathcal{Z}_k(\Phi) \partial_\mu \Phi \cdot \partial_\mu \Phi + \mathcal{O}(\partial^4) \right]. \quad (25)$$

U_k is the scale-dependent effective potential, \mathcal{Z}_k symbolizes the wave-function renormalization associated to the scaling of the kinetic part. The LPA assumes the wave-function renormalization in the derivative expansion (25) to be field-independent and fixed to its initial value of one, $\mathcal{Z}_k(\Phi) = \mathcal{Z}_k = 1$, which corresponds to a vanishing anomalous dimension. Momentum-dependent interactions are neglected in LPA. In the case of the eLSM, the second term in Eq. (25) is given by the kinetic terms of spin-zero and spin-one fields (modified by Stueckelberg's Lagrangian):

$$\Gamma_k[\phi_i, \mathcal{A}_i] = \int_x \left[\frac{1}{2} \partial_\mu \phi_i \partial_\mu \phi_i + \frac{1}{4} \mathcal{F}_{i,\mu\nu} \mathcal{F}_{i,\mu\nu} + \frac{\lambda_{\text{St}}}{2} (\partial_\mu \mathcal{A}_{i,\mu})^2 + U_k(\phi_i, \mathcal{A}_i) \right], \quad (26)$$

$\mathcal{F}_{i,\mu\nu} = \partial_\mu \mathcal{A}_{i,\nu} - \partial_\nu \mathcal{A}_{i,\mu}$. At nonzero temperature, it is technically advantageous to employ the three-dimensional version of Litim's optimal regulator $\propto (k^2 - \bar{q}^2) \Theta(k^2 - \bar{q}^2)$ [102, 103]. Remembering the above discussion about their various limits, the regulating functions are chosen as:

$$R_k^{\text{S}}(q) = (k^2 - \bar{q}^2) \Theta(k^2 - \bar{q}^2), \quad (27)$$

$$R_{k,\mu\nu}^{\text{V}}(q) = [\Pi_{\mu\nu}^{\text{T}}(q) + \lambda_{\text{St}} \Pi_{\mu\nu}^{\text{L}}(q)] (k^2 - \bar{q}^2) \Theta(k^2 - \bar{q}^2), \quad (28)$$

where we have defined the transversal and longitudinal projection operators $\Pi_{\mu\nu}^{\text{T}}(q) = \delta_{\mu\nu} - q_\mu q_\nu / q^2$ and $\Pi_{\mu\nu}^{\text{L}}(q) = q_\mu q_\nu / q^2$, respectively. Since $\partial_k \Gamma_k = \mathcal{V} \partial_k U_k$ for spatially uniform field configurations $\Phi_i(x) = \Phi_i$, and since in the limit $V \rightarrow \infty$ we have $1/V \sum_{\vec{q}} \rightarrow \int d^3q / (2\pi)^3$, using Eq. (27) as well as Eq. (28), Eq. (23) becomes:

$$\partial_k U_k = T \sum_n \int_{V(k)} \frac{d^3q}{(2\pi)^3} k \left\{ \text{tr} \bar{\mathbf{G}}_k^{\text{S}}(\omega_n, \vec{q}) + [\Pi_{\mu\nu}^{\text{T}}(q) + \lambda_{\text{St}} \Pi_{\mu\nu}^{\text{L}}(q)] \text{tr} \bar{\mathbf{G}}_{k,\nu\mu}^{\text{V}}(\omega_n, \vec{q}) \right\}, \quad (29)$$

where $\bar{\mathbf{G}} = \mathcal{V} \mathbf{G}$ and $V(k)$ denotes the spherical volume with radius k in three-momentum space.

3 Results

In this section, we numerically solve the FRG flow equations in LPA for the eLSM introduced in Sec. 2.1 for three scenarios: (i) the $U(2)_R \times U(2)_L$ -symmetric case, (ii) the case with $U(1)_A$ anomaly, and (iii) the case with $U(1)_A$ anomaly and ESB. To this end, we discuss the expansion of the potential U_k in terms of the respective invariants under the given symmetry and fix the bare couplings in the UV such that the renormalization flow produces reasonable values for the physical observables in the IR. From the behavior of the chiral order parameter $\langle \sigma \rangle_0$ as a function of temperature we infer the order of the phase transition and illustrate the restoration of chiral symmetry by computing various mesonic screening masses.

Let us remark that there are, in principle, two different strategies to proceed [47]. In the first strategy one expands the potential U_k around a (local) minimum. The advantage of this method is that one has to solve only a few flow equations (one for each coupling and an additional one for the scale-dependent order parameter). In doing so, however, we can only deduce the potential right at a local minimum. It is not clear whether this local minimum is also the global one. Especially in the case of a first-order transition with two emerging minima, it is crucial not just to know the potential at the expansion point but also at any other local extremum.

To overcome this difficulty, in this paper we follow the second strategy, where U_k is discretized on a grid. Here we gain information about the entire form of the potential, but this strategy needs a lot of computational power as we have to solve flow equations for each grid point. Nevertheless, we utilize this approach because it allows us to figure out the transition order in a comparatively quick and

uncomplicated fashion. We tune the potential in such a way that the physical configuration is located at $\langle \sigma \rangle_0 = \sqrt{Z_\pi} f_\pi$ for $k \rightarrow 0$.

Remember also that the effective action Γ_k is a functional of the classical fields $\phi_{k,i} = \langle \varphi_i \rangle$ and $\mathcal{A}_{k,i,\mu} = \langle A_{i,\mu} \rangle$, cf. Eq. (22), but for the sake of simplicity the brackets indicating expectation values will be omitted in the following, e.g. $\langle \eta \rangle \rightarrow \eta$. Another point is that we are setting certain fields to zero after the calculation of $\Gamma_k^{(2)}$, since we only need to consider as many fields to be non-vanishing as there are independent invariants.

3.1 Chiral limit without anomaly

For zero quark masses and in the absence of $U(1)_A$ -symmetry breaking ($h_0^0 = 0$ as well as $c_A = 0$), the Lagrangian (4) is invariant under the full $U(2)_R \times U(2)_L$ symmetry. In the LPA neither wavefunction renormalization nor momentum-dependent interactions are taken into account. Since the involved (axial-)vector mesons typically have a mass of $\lesssim 1.2$ GeV, an ultraviolet cutoff of $\Lambda = 1.2$ GeV is chosen. After substituting the fields by their expectation values, in compliance with Eq. (26) we derive from Eq. (4) the following effective average action at the UV scale:

$$\begin{aligned} \Gamma_\Lambda = \int_x \left\{ \frac{1}{2} \partial_\mu \sigma \partial_\mu \sigma + \frac{1}{2} \partial_\mu \vec{a}_0 \cdot \partial_\mu \vec{a}_0 + \frac{1}{2} \partial_\mu \eta \partial_\mu \eta + \frac{1}{2} \partial_\mu \vec{\pi} \cdot \partial_\mu \vec{\pi} + \frac{1}{4} (\partial_\mu \omega_\nu - \partial_\nu \omega_\mu)^2 + \frac{1}{4} (\partial_\mu \vec{\rho}_\nu - \partial_\nu \vec{\rho}_\mu)^2 \right. \\ \left. + \frac{1}{4} (\partial_\mu f_{1\nu} - \partial_\nu f_{1\mu})^2 + \frac{1}{4} (\partial_\mu \vec{a}_{1\nu} - \partial_\nu \vec{a}_{1\mu})^2 + \frac{\lambda_{\text{St}}}{2} \left[(\partial_\mu \omega_\mu)^2 + (\partial_\mu \vec{\rho}_\mu)^2 + (\partial_\mu f_{1\mu})^2 + (\partial_\mu \vec{a}_{1\mu})^2 \right] \right. \\ \left. + c_{1,\Lambda} \xi_1 + c_{2,\Lambda} \xi_1^2 + c_{3,\Lambda} \xi_2 + c_{4,\Lambda} \xi_3 + c_{5,\Lambda} \xi_4 \right\}. \end{aligned} \quad (30)$$

In Eq. (30) we have introduced the $O(8)$ mass invariants ξ_1 and ξ_4 as well as the other $U(2)_R \times U(2)_L$ -symmetric expressions ξ_2, ξ_3 contained in Eq. (4). They are linear combinations of the different interaction terms in the effective potential, namely:

$$\xi_1 = \sigma^2 + \vec{a}_0^2 + \eta^2 + \vec{\pi}^2, \quad (31)$$

$$\xi_2 = (\sigma^2 + \vec{\pi}^2) (\eta^2 + \vec{a}_0^2) - (\sigma\eta - \vec{\pi} \cdot \vec{a}_0)^2, \quad (32)$$

$$\begin{aligned} \xi_3 = (\vec{\pi} \cdot \vec{a}_{1\mu} + \eta f_{1\mu})^2 + (\vec{a}_0 \cdot \vec{a}_{1\mu} + \sigma f_{1\mu})^2 \\ + (\vec{\rho}_\mu \times \vec{a}_0 + \eta \vec{a}_{1\mu} + \vec{\pi} f_{1\mu})^2 + (\vec{\pi} \times \vec{\rho}_\mu + \sigma \vec{a}_{1\mu} + \vec{a}_0 f_{1\mu})^2, \end{aligned} \quad (33)$$

$$\xi_4 = f_{1\mu}^2 + \vec{a}_{1\mu}^2 + \omega_\mu^2 + \vec{\rho}_\mu^2. \quad (34)$$

The scale-dependent couplings are defined as:

$$c_{1,k} = \frac{m_{0,k}^2}{2}, \quad c_{2,k} = \frac{1}{4} \left(\lambda_{1,k} + \frac{1}{2} \lambda_{2,k} \right), \quad c_{3,k} = \frac{\lambda_{2,k}}{2}, \quad c_{4,k} = \frac{g_{1,k}^2}{2}, \quad c_{5,k} = \frac{m_{1,k}^2}{2}. \quad (35)$$

For the expansion of U_k we have to replace all non-vanishing field variables by appropriate expressions of the invariants $\{\xi_1, \xi_2, \xi_3, \xi_4\}$. In order to do this, we keep the fields σ , a_0^1 , a_{10}^1 , and ρ_0^1 nonzero. All others are set to zero. Solving the four Eqs. (31) – (34) for these four variables yields:

$$\begin{aligned} \sigma^2 = \frac{1}{2} \left(\xi_1 + \sqrt{\xi_1^2 - 4\xi_2} \right), \quad (a_0^1)^2 = \frac{1}{2} \left(\xi_1 - \sqrt{\xi_1^2 - 4\xi_2} \right), \\ (a_{10}^1)^2 = \frac{\xi_3}{\xi_1}, \quad (\rho_0^1)^2 = \xi_4 - \frac{\xi_3}{\xi_1}. \end{aligned} \quad (36)$$

At first glance, this mapping seems to be singular for $\xi_1 \rightarrow 0$, but we have checked that all parts of the flow equations $\propto \xi_1^{-1}$ cancel for $\xi_1 = 0$, cf. also Refs. [63, 104]. Furthermore, the mapping does not preserve Euclidean invariance, since we keep only the $\mu = 0$ -component of the vector fields ρ_μ^1 and $a_{1\mu}^1$. This gives rise to unequal screening masses of some vector components with differences $\propto \xi_2, \xi_3$, or ξ_4 , but this is also not relevant since we assume that only the sigma field acquires a non-vanishing vacuum expectation value (and hence $\xi_1 \rightarrow \xi_{10} \equiv \sigma_0^2$ and $\xi_2, \xi_3, \xi_4 \rightarrow 0$). This means that we are concerned with

a one-dimensional investigation along the ξ_1 -axis and that, in this limit, Euclidean symmetry is restored again.

Without axial anomaly and quark masses, we expect the chiral phase transition to be of first order as argued in Ref. [17] (among many other studies) and summarized by the ‘‘Columbia plot’’ [105, 106]. Since ξ_2 , ξ_3 , and ξ_4 are set to zero in the end, it is reasonable to truncate U_k at linear order in these invariants (although the flow equation generates terms of arbitrary order in these invariants), with coefficients that are functions of ξ_1 :

$$U_k(\xi_1, \xi_2, \xi_3, \xi_4) = V_k(\xi_1) + W_k(\xi_1)\xi_2 + X_k(\xi_1)\xi_3 + Y_k(\xi_1)\xi_4 . \quad (37)$$

The physical vacuum is specified by the condition $\partial U_k / \partial \sigma = 0$ for $\sigma = \sigma_0$, and the squared mass of the σ field is identical to the curvature of the effective potential:

$$\left. \frac{\partial U_k}{\partial \sigma} \right|_{\sigma=\sigma_0} = 2\sqrt{\xi_{10}} V_k'(\xi_{10}) = 0 , \quad (38)$$

$$\left. \frac{\partial^2 U_k}{\partial \sigma^2} \right|_{\sigma=\sigma_0} = 2V_k''(\xi_{10}) + 4\xi_{10} V_k'''(\xi_{10}) . \quad (39)$$

From Eq. (38) one sees that, for $\xi_{10} \neq 0$, the minimum of the effective potential can also be determined from the condition $V_k' = 0$. Once the system changes to the restored phase ($\sigma_0^2 = \xi_{10} = 0$), V_k' can be nonzero, though.

The explicit flow equations for V_k , W_k , X_k , and Y_k are obtained by differentiating Eq. (29) and evaluating it for the physical configuration:

$$\partial_k V_k(\xi_1) = \partial_k U_k(\xi_1, \xi_2, \xi_3, \xi_4)|_{\xi_2, \xi_3, \xi_4=0} \equiv \frac{1}{2} \text{tr}(\mathbf{G}_k \partial_k \mathbf{R}_k)|_{\xi_2, \xi_3, \xi_4=0} , \quad (40)$$

$$\partial_k W_k(\xi_1) = \partial_k \partial_{\xi_2} U_k(\xi_1, \xi_2, \xi_3, \xi_4)|_{\xi_2, \xi_3, \xi_4=0} \equiv \frac{1}{2} \mathcal{V} \text{tr} \left(-\mathbf{G}_k \Gamma_{k, \xi_2}^{(3)} \mathbf{G}_k \partial_k \mathbf{R}_k \right) \Big|_{\xi_2, \xi_3, \xi_4=0} , \quad (41)$$

$$\partial_k X_k(\xi_1) = \partial_k \partial_{\xi_3} U_k(\xi_1, \xi_2, \xi_3, \xi_4)|_{\xi_2, \xi_3, \xi_4=0} \equiv \frac{1}{2} \mathcal{V} \text{tr} \left(-\mathbf{G}_k \Gamma_{k, \xi_3}^{(3)} \mathbf{G}_k \partial_k \mathbf{R}_k \right) \Big|_{\xi_2, \xi_3, \xi_4=0} , \quad (42)$$

$$\partial_k Y_k(\xi_1) = \partial_k \partial_{\xi_4} U_k(\xi_1, \xi_2, \xi_3, \xi_4)|_{\xi_2, \xi_3, \xi_4=0} \equiv \frac{1}{2} \mathcal{V} \text{tr} \left(-\mathbf{G}_k \Gamma_{k, \xi_4}^{(3)} \mathbf{G}_k \partial_k \mathbf{R}_k \right) \Big|_{\xi_2, \xi_3, \xi_4=0} . \quad (43)$$

The equation for V_k turns out to be equivalent to the flow equation for free fields, as interactions are no longer present for $\xi_2, \xi_3, \xi_4 = 0$:

$$\begin{aligned} \partial_k V_k(\xi_1) = \frac{Tk^4}{6\pi^2} \sum_n \left[\frac{4}{\omega_n^2 + k^2 + 2V_k'} + \frac{1}{\omega_n^2 + k^2 + 2V_k' + 4\xi_1 V_k''} + \frac{3}{\omega_n^2 + k^2 + 2V_k' + 2\xi_1 W_k} \right. \\ \left. + \frac{12}{\omega_n^2 + k^2 + 2Y_k} + \frac{12}{\omega_n^2 + k^2 + 2(Y_k + \xi_1 X_k)} \right. \\ \left. + \frac{4}{\omega_n^2 + k^2 + 2Y_k/\lambda_{\text{St}}} + \frac{4}{\omega_n^2 + k^2 + 2(Y_k + \xi_1 X_k)/\lambda_{\text{St}}} \right] . \end{aligned} \quad (44)$$

Here, explicit ξ_1 -dependences on the right-hand side are implied. The masses of the fields ρ and ω as well as f_1 and a_1 are equal in the presence of $SU(2)_V$ invariance. Equation (44) reveals some characteristics of the considered model: the $4 + 1 + 3 = 8$ (pseudo-)scalar degrees of freedom are represented by the first line. The first term of Eq. (44) corresponds to the mass-degenerate η and $\vec{\pi}$. The second and the third describe the σ and the \vec{a}_0 , respectively. As a cross-check, note that the mass eigenvalues of these spin-zero fields are equal to the ones quoted in Ref. [63]. The second line corresponds to the physical degrees of freedom of the (axial-)vector mesons ($(4 \times 3) + (4 \times 3) = 12 + 12$ fields), whereas the last line corresponds to their unphysical degrees of freedom ($4 + 4$) introduced via Stueckelberg’s Lagrangian. Obviously, these eight additional degrees of freedom decouple from the flow for $\lambda_{\text{St}} \rightarrow 0$. The Matsubara sum over n can be carried out analytically, e.g. by a contour integral in the complex plane [107]. The flow of $V_k(\xi_1)$ entangles with the flow of $W_k(\xi_1)$, $X_k(\xi_1)$, and $Y_k(\xi_1)$. Thus the flow equations for these coefficients are necessary to obtain a closed set of differential equations. For the sake of clarity, they are presented in Appendix A.

Figure 1 **A** summarizes the dependence of σ_0 on T . The order parameter σ_0 becomes successively smaller and drops discontinuously to zero at $T_c \simeq 147.4$ MeV, indicating a first-order phase transition. The discontinuity occurring at this temperature is marked with a dashed line. Figure 1 **B** demonstrates how, as the temperature increases, the mesonic screening masses of chiral partners approach each other. These are (i) ρ and a_1 , (ii) ω and f_1 (their masses are not shown explicitly, since $m_\omega = m_\rho$ and $m_{f_1} = m_{a_1}$), (iii) σ and π , as well as (iv) a_0 and η ($m_\eta = m_\pi$, thus we do not show m_η explicitly). The masses of chiral partners become degenerate at the transition temperature and above. Note that solid lines correspond to data interpolated using cubic splines. In cases where the data points are explicitly given in terms of colored crosses, however, the lines represent a cubic smoothing spline fit. Details are provided in Appendix B.

The ρ/a_1 mass increases/decreases before the transition point is reached. Pions and η are the Goldstone bosons of chiral symmetry breaking, and thus necessarily massless in the broken phase. This is explained by Eq. (38): if $\xi_{10} \neq 0$, the physical minimum is located at the point where $V'_k(\xi_1) = 0$. Inspecting Eq. (44), we see that V'_k is indeed proportional to the (squared) mass of pion and η . However, for $T > T_c$ the ground state is characterized by $\xi_{10} = 0$, and thus $V'_k(0)$ (i.e., the masses of pions and η) may differ from zero.

We tuned the UV-parameters in the vacuum to achieve the most “realistic” mesonic screening masses and a nonzero value for σ_0 of around 147.9 MeV (the tree-level value is $\sigma_0 = \sqrt{Z_\pi} f_\pi \simeq 148.8$ MeV). Apparently, the IR vacuum masses of the σ and a_0 mesons are far too small compared to what we expect from the PDG [90], no matter whether we choose the assignment $\{f_0(500), a_0(980)\}$ or $\{f_0(1370), a_0(1450)\}$. We will return to a discussion of this issue below. Furthermore, the masses of ω and ρ are too heavy. The ratio between the masses of ρ and a_1 is smaller than expected (experimentally it should be around 1.6).

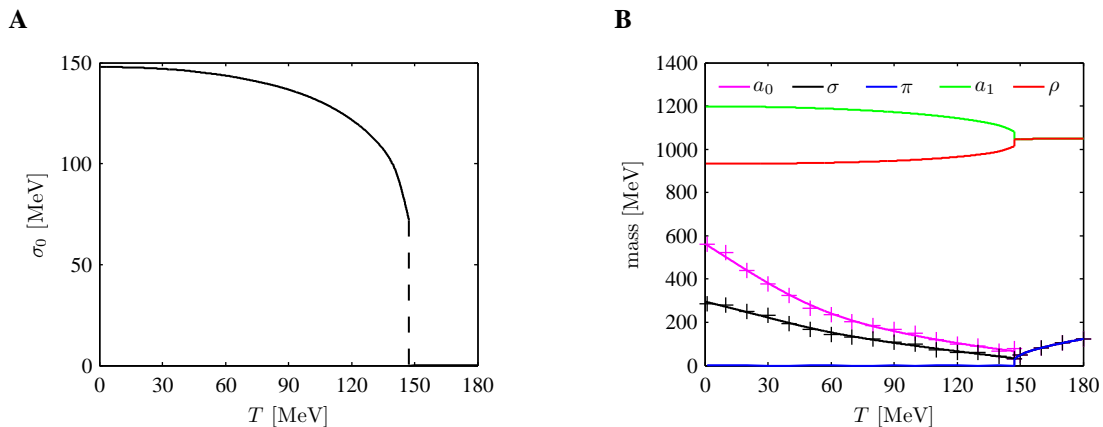


Figure 1: Phase transition in the eLSM with $U(2)_R \times U(2)_L$ symmetry. **A** Order parameter σ_0 as a function of temperature. **B** Screening masses as a function of temperature.

3.2 Chiral limit with $U(1)_A$ anomaly

As a second scenario we want to study how the $U(1)_A$ anomaly influences the order of the transition and the mesonic masses. The coupling c_A in Eq. (4) is now nonzero and quantifies the strength of the $U(1)_A$ -symmetry breaking. Proceeding similarly as above, Γ_Λ is slightly modified:

$$\Gamma_\Lambda = \int_x \left\{ \frac{1}{2} \partial_\mu \sigma \partial_\mu \sigma + \frac{1}{2} \partial_\mu \vec{a}_0 \cdot \partial_\mu \vec{a}_0 + \frac{1}{2} \partial_\mu \eta \partial_\mu \eta + \frac{1}{2} \partial_\mu \vec{\pi} \cdot \partial_\mu \vec{\pi} + \frac{1}{4} (\partial_\mu \omega_\nu - \partial_\nu \omega_\mu)^2 + \frac{1}{4} (\partial_\mu \vec{\rho}_\nu - \partial_\nu \vec{\rho}_\mu)^2 \right. \\ \left. + \frac{1}{4} (\partial_\mu f_{1\nu} - \partial_\nu f_{1\mu})^2 + \frac{1}{4} (\partial_\mu \vec{a}_{1\nu} - \partial_\nu \vec{a}_{1\mu})^2 + \frac{\lambda_{\text{St}}}{2} \left[(\partial_\mu \omega_\mu)^2 + (\partial_\mu \vec{\rho}_\mu)^2 + (\partial_\mu f_{1\mu})^2 + (\partial_\mu \vec{a}_{1\mu})^2 \right] \right. \\ \left. + \bar{c}_{1,\Lambda} \bar{\xi}_1 + \bar{c}_{2,\Lambda} \bar{\xi}_1^2 + \bar{c}_{3,\Lambda} \bar{\xi}_1 \bar{\xi}_2 + \bar{c}_{4,\Lambda} \bar{\xi}_2 + \bar{c}_{5,\Lambda} \bar{\xi}_2^2 + \bar{c}_{6,\Lambda} \bar{\xi}_3 + c_{4,\Lambda} \xi_3 + c_{5,\Lambda} \xi_4 \right\}, \quad (45)$$

with the new invariants $\bar{\xi}_1, \bar{\xi}_2, \bar{\xi}_3$:

$$\bar{\xi}_1 = \sigma^2 + \bar{\pi}^2, \quad (46)$$

$$\bar{\xi}_2 = \eta^2 + \bar{a}_0^2, \quad (47)$$

$$\bar{\xi}_3 = (\sigma\eta - \bar{\pi} \cdot \bar{a}_0)^2. \quad (48)$$

The former invariants ξ_1 and ξ_2 are functions of the new invariants $\bar{\xi}_1, \bar{\xi}_2$, and $\bar{\xi}_3$: $\xi_1 = \bar{\xi}_1 + \bar{\xi}_2$, $\xi_2 = \bar{\xi}_1\bar{\xi}_2 - \bar{\xi}_3$. The origin of the new invariants is the $U(1)_A$ -symmetry breaking term $\sim \det \Sigma + \det \Sigma^\dagger$ in Eq. (4). The invariants ξ_3 and ξ_4 remain unchanged. The scale-dependent couplings of the effective potential are now defined as follows:

$$\begin{aligned} \bar{c}_{1,k} &= \frac{1}{2} (m_{0,k}^2 - c_{A,k}), & \bar{c}_{2,k} &= \frac{1}{4} \left(\lambda_{1,k} + \frac{1}{2} \lambda_{2,k} \right), & \bar{c}_{3,k} &= \frac{1}{2} \left(\lambda_{1,k} + \frac{3}{2} \lambda_{2,k} \right), \\ \bar{c}_{4,k} &= \frac{1}{2} (m_{0,k}^2 + c_{A,k}), & \bar{c}_{5,k} &= \frac{1}{4} \left(\lambda_{1,k} + \frac{1}{2} \lambda_{2,k} \right), & \bar{c}_{6,k} &= -\frac{\lambda_{2,k}}{2}, \\ c_{4,k} &= \frac{g_{1,k}^2}{2}, & c_{5,k} &= \frac{m_{1,k}^2}{2}. \end{aligned} \quad (49)$$

We again want to expand U_k in terms of $\bar{\xi}_1, \dots, \xi_4$. For five different invariants we have to keep at least five fields nonzero. In addition to σ, a_0^1, a_{10}^1 , and ρ_0^1 we decided to take the η field into account and map those variables onto the set $\{\bar{\xi}_1, \bar{\xi}_2, \bar{\xi}_3, \xi_3, \xi_4\}$:

$$\sigma^2 = \bar{\xi}_1, \quad (a_0^1)^2 = \bar{\xi}_2 - \frac{\bar{\xi}_3}{\bar{\xi}_1}, \quad \eta^2 = \frac{\bar{\xi}_3}{\bar{\xi}_1}, \quad (a_{10}^1)^2 = \frac{\xi_3}{\bar{\xi}_1 + \xi_2}, \quad (\rho_0^1)^2 = \xi_4 - \frac{\xi_3}{\bar{\xi}_1 + \xi_2}. \quad (50)$$

Similarly to Sec. 3.1, the potential is now discretized with respect to $\bar{\xi}_1$ and one assumes that the physical minimum is attained for $\bar{\xi}_{10} \equiv \sigma_0^2$ and $\bar{\xi}_2, \bar{\xi}_3 = 0$. Thus, in the ansatz for the effective potential, we restrict ourselves to the linear order in $\bar{\xi}_2, \bar{\xi}_3, \xi_3$, and ξ_4 :

$$U_k(\bar{\xi}_1, \bar{\xi}_2, \bar{\xi}_3, \xi_3, \xi_4) = \bar{V}_k(\bar{\xi}_1) + \bar{W}_k(\bar{\xi}_1)\bar{\xi}_2 + \bar{X}_k(\bar{\xi}_1)\bar{\xi}_3 + \bar{Y}_k(\bar{\xi}_1)\xi_3 + \bar{Z}_k(\bar{\xi}_1)\xi_4. \quad (51)$$

The flow equation for $\bar{V}_k(\bar{\xi}_1)$ reads:

$$\begin{aligned} \partial_k \bar{V}_k(\bar{\xi}_1) &= \frac{Tk^4}{6\pi^2} \sum_n \left[\frac{3}{\omega_n^2 + k^2 + 2\bar{V}_k'} + \frac{1}{\omega_n^2 + k^2 + 2\bar{V}_k' + 4\bar{\xi}_1\bar{V}_k''} + \frac{3}{\omega_n^2 + k^2 + 2\bar{W}_k} \right. \\ &\quad + \frac{1}{\omega_n^2 + k^2 + 2(\bar{W}_k + \bar{\xi}_1\bar{X}_k)} + \frac{12}{\omega_n^2 + k^2 + 2\bar{Z}_k} + \frac{12}{\omega_n^2 + k^2 + 2(\bar{Z}_k + \bar{\xi}_1\bar{Y}_k)} \\ &\quad \left. + \frac{4}{\omega_n^2 + k^2 + 2\bar{Z}_k/\lambda_{\text{St}}} + \frac{4}{\omega_n^2 + k^2 + 2(\bar{Z}_k + \bar{\xi}_1\bar{Y}_k)/\lambda_{\text{St}}} \right]. \end{aligned} \quad (52)$$

Note that the η meson now attains a mass different from that of the pions: it becomes massive in the spontaneously broken phase, as it should be, since $U(1)_A$ is explicitly broken and there are only three (and no longer four) Goldstone bosons.

Again we tune the bare parameters such that most realistic meson masses are obtained in the IR. The order parameter σ_0 continuously decreases with increasing T , until it vanishes at a critical temperature of approximately 276.5 MeV, see Fig. 2 **A**. We conclude that the axial anomaly turns the first-order transition, found in the $U(2)_R \times U(2)_L$ -symmetric theory, into a second-order phase transition with a significantly higher critical temperature. Figure 2 **B** shows the evolution of the masses of (pseudo)-scalar and (axial)-vector mesons. Again, there are four different pairs of chiral partners, (ρ, a_1) , (ω, f_1) (the masses of which are identical to the corresponding mesons in the first pair and thus not shown explicitly), (σ, π) , as well as (η, a_0) . The masses of chiral partners become degenerate at the transition temperature. The pions assume a non-vanishing mass above the critical temperature for the same reason as discussed in the previous section. At zero temperature, the $\rho(\omega)$ meson mass is close to its physical value, but the $a_1(f_1)$ mass is too small. The mass difference between vector (ω, ρ) and axial-vector mesons (f_1, a_1) comes out to be $\simeq 268.7$ MeV and is of the same magnitude as for the $U(2)_R \times U(2)_L$ -symmetric case ($\simeq 265.4$ MeV). The η -meson mass is too large, but remember that the η in our case consists only of

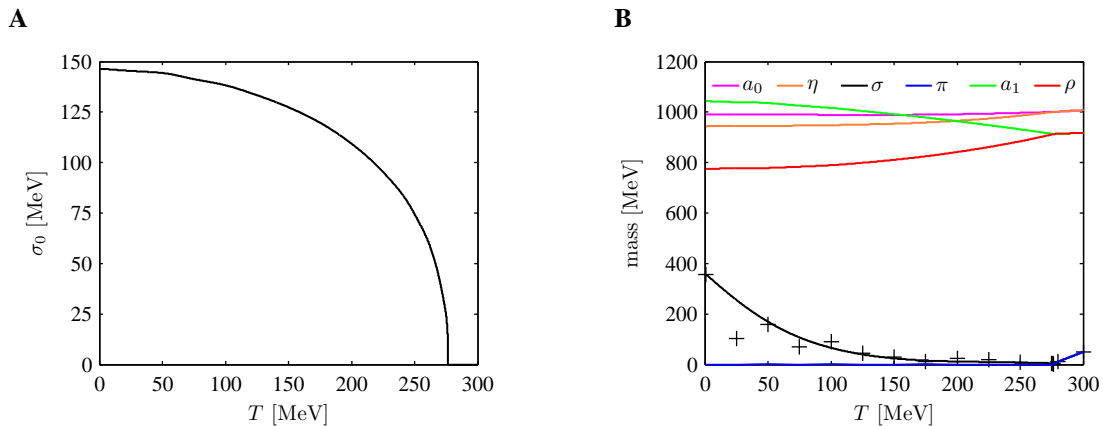


Figure 2: Phase transition in the eLSM with $SU(2)_V \times SU(2)_A \times U(1)_V$ symmetry. **A** Order parameter σ_0 as a function of the temperature T . **B** Screening masses as a function of temperature.

nonstrange quarks, while the physical η is an admixture of nonstrange and strange quarks. The vacuum mass of the σ of around 357.4 MeV is now only slightly smaller than the experimental value for the mass of $f_0(500)$, while the vacuum mass of a_0 is very close to its experimental value. The data points for the mass of the σ fluctuate strongly as a function of temperature, since the potential is rather flat in this case and its curvature (the squared σ mass) is rather hard to determine numerically with reasonable accuracy.

3.3 Explicitly broken chiral symmetry with anomaly

Finally, we apply our FRG analysis to the case of ESB due to nonzero and degenerate quark masses ($h_0^0 \neq 0$). The truncation of the effective potential (51) is still valid. In the case of ESB, the root of \bar{V}'_k no longer coincides with the one of $\partial U_k / \partial \sigma$ for nonzero vacuum expectation values of the σ field. The global minimum $\bar{\xi}_{10}$ must now fulfill the following relation:

$$2\sqrt{\bar{\xi}_{10}}\bar{V}'_k(\bar{\xi}_{10}) - h_0^0 = 0, \quad (53)$$

i.e., the expansion coefficients \bar{W}_k , \bar{X}_k , etc., are evaluated for a shifted $\bar{\xi}_{10}$, producing massive pseudo-Goldstone bosons π (which have a nonzero mass even for $\sigma_0 \neq 0$).

According to Eq. (53), the potential never has a global minimum at $\bar{\xi}_1 = 0$. Solving the flow equations on the $\bar{\xi}_1$ grid, the results are shown in Fig. 3. In Fig. 3 **A**, we see that σ_0 decreases and tends asymptotically towards zero. Consequently, the transition is a crossover transition. At an estimated pseudocritical temperature of $T_{pc} \simeq 354.8$ MeV, the curvature changes its sign. Figure 3 **B** reveals that, with the choice $h_0^0 = 3 \times 10^6$ MeV³, the pions exhibit a nonzero mass of $\simeq 142.5$ MeV in vacuum. The masses of chiral partners approach each other, but do not become identical. We further observe a dropping a_1 meson mass but an increasing ρ mass. The vacuum σ mass of 598.5 MeV is a little larger than the physical value for the $f_0(500)$ resonance. The remaining masses are in good agreement with the results of Sec. 3.2. The gap between the masses of the ρ and a_1 mesons is now 314.5 MeV (compared to 268.7 MeV in the previous case).

4 Summary and Outlook

The QCD transition is commonly associated with the restoration of chiral symmetry. Experimentally, this could be detected by a change of the in-medium masses of (axial-)vector mesons. It is therefore essential to include them in a theoretical analysis. Non-perturbative continuum methods, such as the FRG, provide new insights into the QCD transition, as they do not rely on weak couplings and are applicable at nonzero net-baryon density where lattice QCD suffers from the fermion-sign problem.

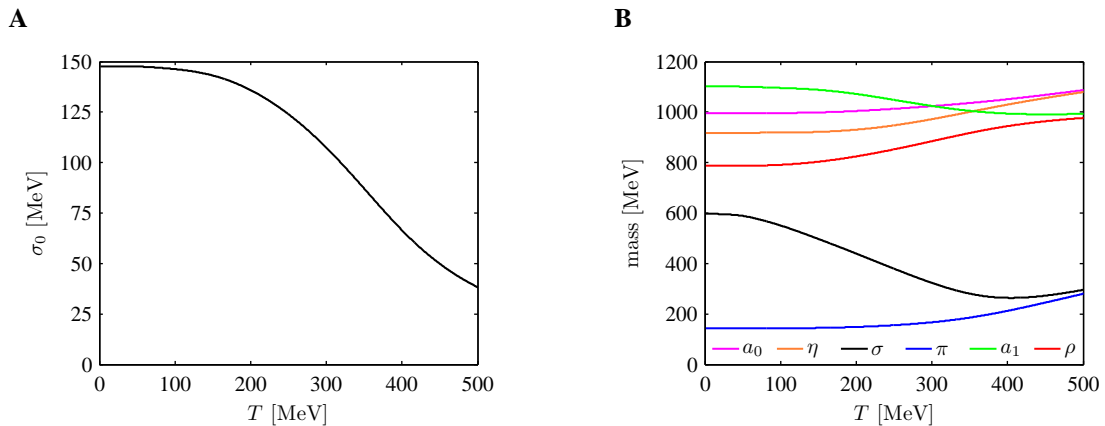


Figure 3: Phase transition in the eLSM with ESB and $U(1)_A$ anomaly. **A** Order parameter σ_0 as a function of temperature. **B** Screening masses as a function of temperature.

In this study, we investigated the chiral transition for two flavors by applying the FRG formalism to the eLSM, an effective low-energy model for QCD. Thus, our work is an extension of many studies involving two-flavor effective models for QCD, see e.g. Refs. [18, 63, 64], in the sense that vector and axial-vector mesonic degrees of freedom are now incorporated into the FRG flow. In order to derive the FRG flow equations with (axial-)vector mesons, Stueckelberg’s Lagrangian has been employed [98, 99, 100]. We use the grid method and the LPA to compute the flow of the effective potential. The order of the phase transition and the meson screening masses were determined in three different scenarios: (i) the chiral limit without $U(1)_A$ anomaly, (ii) the chiral limit with $U(1)_A$ anomaly, and (iii) the realistic case with nonvanishing quark masses and $U(1)_A$ anomaly.

Overall, our numerical results are broadly consistent with previous findings. Regarding the full $U(2)_R \times U(2)_L$ -symmetric theory, cf. Sec. 3.1, our conclusion is compatible with Ref. [64] and the statement of Pisarski and Wilczek [17] that the chiral phase transition is of first order for $N_f = 2$ and massless quarks. Reducing the symmetry to $SU(2)_V \times SU(2)_A \times U(1)_V$ (Sec. 3.2) turns it into a second-order transition, which is also in agreement with Ref. [17] as well as with the three-flavor study of Ref. [60]. Explicitly breaking chiral symmetry to an exact isospin symmetry generates a crossover transition (Sec. 3.3).

In comparison with the results from the CJT formalism [81] or lattice-QCD simulations [22, 23, 108], the pseudocritical temperature $T_{pc} \simeq 354.8$ MeV of the crossover transition comes out larger, cf. $T_{pc} \simeq 195$ MeV resp. 155 MeV in the aforementioned approaches. It is conceivable that this deviation arises from the lack of quark fields in our approach, which, being rather light degrees of freedom, evidently contribute substantially to the FRG flow [75], and from the fact that presently our approach ignores momentum-dependent vertices and interactions among (axial-) vector mesons. It has to be clarified how higher orders in the derivative expansion affect the transition. We hope that by additional investigations, as stated below, we are able to improve our results.

In all three scenarios studied here, it was demonstrated how the masses of chiral partners become degenerate at the phase boundary and beyond, see Figs. 1 **B**, 2 **B**, and 3 **B**. The mass degeneracy is a necessary condition for the restoration of chiral symmetry [6, 7, 8, 9]. Let us note that in our study the mass of the a_1 mass decreases towards the chiral transition, but not the mass of the ρ , cf. Fig. 3 **B**. In the CJT study of Ref. [81] the authors also found an increasing ρ mass towards the chiral transition. In principle, Ref. [6] argues that the ρ meson mass has to increase in the framework of a gauged two-flavor LSM, but a globally symmetric LSM could also allow for a dropping ρ mass.

In the physically most realistic scenario with ESB and $U(1)_A$ anomaly, the vacuum masses of (σ, a_0) come out to be (598.5, 996.3) MeV. This is in the range of the masses of the light scalar resonances $\{f_0(500), a_0(980)\}$. However, Refs. [76, 77, 78] suggested that the chiral partners of π and η should be $\{f_0(1370), a_0(1450)\}$. This seems to be a natural scenario, if the latter are (predominantly) quark-antiquark states. Then, the light resonances $\{f_0(500), a_0(980)\}$ are most likely made of four quarks, e.g. in the form of resonances in the scattering continuum, or even bound states, of two pseudoscalar mesons.

Also bound states of diquark and anti-diquark molecules have been suggested to explain their nature. As suggested a long time ago by Jaffe [109], this "tetraquark" interpretation of the light scalar resonances would naturally explain the "inverse mass ordering" of these states. By construction, the FRG approach resums correlations of infinite order and thus, if $\{f_0(500), a_0(980)\}$ are correlated states of pseudoscalar mesons, would naturally generate these mesons dynamically. This could be an explanation why the masses of σ and a_0 come out close to those of $\{f_0(500), a_0(980)\}$. (In fact, we were not able to find UV-parameters such that the IR vacuum masses of σ and a_0 are close to those of $\{f_0(1370), a_0(1450)\}$.) Note that the chiral transition was studied in the presence of both a light and a heavy scalar state in Ref. [110]. There it was shown that there is actually no conflict with the "tetraquark" scalar state being light and the heavy scalar state being the chiral partner of the pion.

There are many questions left open for future study. E.g. one should investigate the order of the phase transition as a function of the anomaly strength. The first-order transition in Sec. 3.1 should smoothly pass into one of second order, as shown in Sec. 3.2. Moreover, one needs to figure out when exactly the $U(1)_A$ anomaly disappears for high temperatures. This can be done by assuming c_A to be proportional to an explicitly T -dependent instanton density. In order to decide whether the transition lies in the $O(4)$ -universality class or not [17, 18], the critical exponents have to be calculated. A natural next step in our analysis is to account for non-trivial wave-function renormalization factors, i.e., going beyond the LPA. One can readily extend our investigations to $N_f = 3$ quark flavors, but in this case one has an additional order parameter (the strange condensate) which necessitates the use of a two-dimensional grid [60] and thus considerably increases the numerical effort. Baryonic degrees of freedom also play an important role for dilepton production [10]. Therefore, it is mandatory to involve them in the FRG flow. The first candidate for such an extension would be the nucleon and its chiral partner [111, 112] – if the latter exists [113]. As this partner would probably be heavier than the Δ baryons, one should furthermore include spin-3/2 resonances and their chiral partners [114]. Finally, another topic for future studies is to introduce quarks in the FRG. The reason for this is that, as mentioned above, a large contribution to the FRG flow usually comes from the quarks, while the vector and axial-vector mesons are suppressed due to their large mass.

5 Acknowledgments

The authors thank Jan M. Pawłowski, Robert D. Pisarski, Bernd-Jochen Schaefer, Lorenz von Smekal, and Mario Mitter for valuable discussions.

A Flow equations

The flow equations for the expansion coefficients of the effective potential U_k are generally of the form:

$$\partial_k F_{k,i} = \frac{T}{2\pi^2} \sum_n \int_0^k dq \bar{q}^2 f_{k,i}(F_k, F'_k, F''_k, \omega_n^2, \bar{q}^2), \quad (54)$$

with $F_k = (V_k, W_k, \dots)$, $f_k = (v_k, w_k, \dots)$, and $q = |\vec{q}|$. Dependences on $\xi_1, \bar{\xi}_1$ were omitted. The derivatives $F'_k = \partial F_k / \partial \xi_1$ and $F''_k = \partial^2 F_k / (\partial \xi_1)^2$ (or $F'_k = \partial F_k / \partial \bar{\xi}_1$ and $F''_k = \partial^2 F_k / (\partial \bar{\xi}_1)^2$, respectively) are approximated by finite differences, which leads to a solvable system:

$$\partial_k F_{k,i} = \frac{T}{2\pi^2} \sum_n \int_0^k dq \bar{q}^2 f_{k,i}(F_k, \omega_n^2, \bar{q}^2). \quad (55)$$

The functions $f_{k,i}$ are specified in subsections A.1 and A.2. The sum over Matsubara frequencies is performed analytically, e.g.

$$\sum_n \int_0^k dq q^4 \frac{1}{E_\sigma^4(\omega_n^2 + q^2)} = \int_0^k dq q^4 \left[\frac{\coth\left(\frac{q}{2T}\right)}{2qT(k^2 + 4\xi_1 V_k'' + 2V_k' - q^2)^2} \right]$$

$$\begin{aligned}
& \frac{\operatorname{csch}^2\left(\frac{\sqrt{k^2+4\xi_1 V_k''+2V_k'}}{2T}\right)}{8T^2(k^2+4\xi_1 V_k''+2V_k'-q^2)^2} \\
& + \frac{q^2 \operatorname{csch}^2\left(\frac{\sqrt{k^2+4\xi_1 V_k''+2V_k'}}{2T}\right)}{8T^2(k^2+4\xi_1 V_k''+2V_k')(k^2+4\xi_1 V_k''+2V_k'-q^2)^2} \\
& + \frac{q^2 \sinh\left(\frac{\sqrt{k^2+4\xi_1 V_k''+2V_k'}}{T}\right) \operatorname{csch}^2\left(\frac{\sqrt{k^2+4\xi_1 V_k''+2V_k'}}{2T}\right)}{8T(k^2+4\xi_1 V_k''+2V_k')^{3/2}(k^2+4\xi_1 V_k''+2V_k'-q^2)^2} \\
& - \frac{3 \sinh\left(\frac{\sqrt{k^2+4\xi_1 V_k''+2V_k'}}{T}\right) \operatorname{csch}^2\left(\frac{\sqrt{k^2+4\xi_1 V_k''+2V_k'}}{2T}\right)}{8T\sqrt{k^2+4\xi_1 V_k''+2V_k'}(k^2+4\xi_1 V_k''+2V_k'-q^2)^2} \Bigg]. \quad (56)
\end{aligned}$$

Where necessary, the momentum integration is performed by using numerical quadrature.

The potentials V_k and \bar{V}_k are initialized as follows:

$$V_\Lambda(\xi_1) = a_\Lambda (\xi_1 - b_\Lambda)^2, \quad (57)$$

$$\bar{V}_\Lambda(\bar{\xi}_1) = \bar{a}_\Lambda (\bar{\xi}_1 - \bar{b}_\Lambda)^2, \quad (58)$$

where $a_\Lambda = 4.0$, $b_\Lambda = 297.6$ MeV, $\bar{a}_\Lambda = 5.5$, and $\bar{b}_\Lambda = 255.0$ MeV. Furthermore, we have $W_\Lambda(\xi_1) = 30$, $X_\Lambda(\xi_1) = 20$, $Y_\Lambda(\xi_1) = 2.87 \times 10^5$ MeV², $\bar{W}_\Lambda(\bar{\xi}_1) = 2.5 \times 10^5$ MeV², $\bar{X}_\Lambda(\bar{\xi}_1) = -1.0$, $\bar{Y}_\Lambda(\bar{\xi}_1) = 31.0$, and $\bar{Z}_\Lambda = 1.27 \times 10^5$ MeV². Under the assumption of ESB, the UV parameters change to: $\bar{W}_\Lambda(\bar{\xi}_1) = 2.0 \times 10^5$ MeV², $\bar{Y}_\Lambda(\bar{\xi}_1) = 45.0$, and $\bar{Z}_\Lambda = 1.1 \times 10^5$ MeV², while the rest remain identical.

A.1 Flow equations without $U(1)_A$ anomaly

In the case without $U(1)_A$ anomaly, the quantities $f_{k,i}$ in Eq. (55) read

$$v_k = k \left(\frac{3}{E_{a_0}^2} + \frac{12}{E_{a_1}^2} + \frac{12}{E_\rho^2} + \frac{1}{E_\sigma^2} + \frac{4}{E_\pi^2} \right), \quad (59)$$

$$\begin{aligned}
w_k = \frac{1}{2} k \Bigg\{ & - \frac{4 [2V_k'' (8W_k - 3\xi_1 W_k') + 15\xi_1 W_k W_k' + 4\xi_1^2 W_k'^2 + W_k^2]}{E_{a_0}^4 \xi_1 (W_k - 2V_k'')} + \frac{24X_k}{E_{a_1}^4 \xi_1} + \frac{192X_k^2}{E_{a_1}^6} \\
& - \frac{4 [2V_k'' (2\xi_1^2 W_k'' + 9\xi_1 W_k' + 6W_k) + \xi_1 W_k (3W_k' - 2\xi_1 W_k'') + 4\xi_1^2 W_k'^2 + 3W_k^2]}{\xi_1 E_\sigma^4 (2V_k'' - W_k)} \\
& - \frac{8(2\xi_1 W_k' + W_k)}{E_\pi^4 \xi_1} + \frac{16W_k^2}{E_\pi^6} - \frac{24X_k}{\xi_1 E_\rho^4} \Bigg\}, \quad (60)
\end{aligned}$$

$$\begin{aligned}
x_k = \frac{1}{2} k \Bigg\{ & - \frac{16\bar{q}^2 X_k^2}{E_\pi^4 E_{a_1}^2 (\omega_n^2 + \bar{q}^2)} + \frac{32\bar{q}^2 X_k^2}{E_{a_0}^4 E_{a_1}^2 (\omega_n^2 + \bar{q}^2)} - \frac{16\bar{q}^2 X_k^2}{E_\pi^2 E_{a_1}^4 (\omega_n^2 + \bar{q}^2)} + \frac{32\bar{q}^2 X_k^2}{E_{a_0}^2 E_{a_1}^4 (\omega_n^2 + \bar{q}^2)} \\
& + \frac{32\bar{q}^2 (\xi_1 X_k' + X_k + Y_k')^2}{E_{a_1}^2 E_\sigma^4 (\omega_n^2 + \bar{q}^2)} + \frac{32\bar{q}^2 (\xi_1 X_k' + X_k + Y_k')^2}{E_{a_1}^4 E_\sigma^2 (\omega_n^2 + \bar{q}^2)} - \frac{16\bar{q}^2 X_k^2}{E_{a_0}^4 (\omega_n^2 + \bar{q}^2) (\xi_1 X_k + Y_k)} \\
& + \frac{4 \left[X_k \left(\frac{4X_k}{\xi_1 X_k + Y_k} + \frac{1}{\xi_1} \right) - 3X_k' \right]}{E_{a_0}^4} + \frac{16\bar{q}^2 X_k^2}{E_\pi^4 E_\rho^2 (\omega_n^2 + \bar{q}^2)} + \frac{16\bar{q}^2 X_k^2}{E_\pi^2 E_\rho^4 (\omega_n^2 + \bar{q}^2)} \\
& - \frac{16\bar{q}^2 (\xi_1 X_k' + X_k + Y_k')^2}{E_\sigma^4 (\omega_n^2 + \bar{q}^2) (\xi_1 X_k + Y_k)} - \frac{8\xi_1 \bar{q}^2 X_k^3}{E_\pi^4 Y_k (\omega_n^2 + \bar{q}^2) (\xi_1 X_k + Y_k)} - \frac{32\bar{q}^2 Y_k'^2}{E_\rho^4 E_\sigma^2 (\omega_n^2 + \bar{q}^2)} - \frac{32\bar{q}^2 Y_k'^2}{E_\rho^2 E_\sigma^4 (\omega_n^2 + \bar{q}^2)} \\
& + \frac{16\bar{q}^2 Y_k'^2}{E_\sigma^4 Y_k (\omega_n^2 + \bar{q}^2)} + \frac{4 \left[-2\xi_1 X_k'' - \frac{X_k}{\xi_1} + \frac{4(\xi_1 X_k' + X_k + Y_k')^2}{\xi_1 X_k + Y_k} - 5X_k' - \frac{4Y_k'^2}{Y_k} \right]}{E_\sigma^4} \Bigg\}
\end{aligned}$$

$$+ \left. \frac{8 \left(\frac{\xi_1 X_k^3}{\xi_1 X_k Y_k + Y_k^2} - 2X_k' \right)}{E_\pi^4} \right\}, \quad (61)$$

$$y_k = \frac{1}{2} k \left\{ \frac{16\xi_1 \bar{q}^2 X_k^2}{E_\pi^4 E_{a_1}^2 (\omega_n^2 + \bar{q}^2)} + \frac{16\xi_1 \bar{q}^2 X_k^2}{E_\pi^2 E_{a_1}^4 (\omega_n^2 + \bar{q}^2)} - \frac{4(2X_k + 3Y_k')}{E_{a_0}^4} - \frac{8\xi_1 \bar{q}^2 X_k^2}{E_\pi^4 (\omega_n^2 + \bar{q}^2) (\xi_1 X_k + Y_k)} \right. \\ \left. + \frac{32\xi_1 \bar{q}^2 Y_k'^2}{E_\rho^4 E_\sigma^2 (\omega_n^2 + \bar{q}^2)} + \frac{32\xi_1 \bar{q}^2 Y_k'^2}{E_\rho^2 E_\sigma^4 (\omega_n^2 + \bar{q}^2)} - \frac{16\xi_1 \bar{q}^2 Y_k'^2}{E_\sigma^4 Y_k (\omega_n^2 + \bar{q}^2)} + \frac{8 \left(-\frac{X_k Y_k}{\xi_1 X_k + Y_k} - 2Y_k' \right)}{E_\pi^4} \right. \\ \left. - \frac{4 [Y_k (2\xi_1 Y_k'' + Y_k') - 4\xi_1 Y_k'^2]}{E_\sigma^4 Y_k} \right\}, \quad (62)$$

with:

$$E_\sigma^2 = k^2 + \omega_n^2 + 2V_k' + 4\xi_1 V_k'', \quad (63)$$

$$E_\pi^2 = k^2 + \omega_n^2 + 2V_k', \quad (64)$$

$$E_{a_0}^2 = k^2 + \omega_n^2 + 2V_k' + 2\xi_1 W_k, \quad (65)$$

$$E_\rho^2 = k^2 + \omega_n^2 + 2Y_k, \quad (66)$$

$$E_{a_1}^2 = k^2 + \omega_n^2 + 2Y_k + 2\xi_1 X_k. \quad (67)$$

The meson masses are given by:

$$m_\sigma = \sqrt{2V_k' + 4\xi_1 V_k''}, \quad (68)$$

$$m_\pi = \sqrt{2V_k'}, \quad (69)$$

$$m_{a_0} = \sqrt{2V_k' + 2\xi_1 W_k}, \quad (70)$$

$$m_\rho = \sqrt{2Y_k}, \quad (71)$$

$$m_{a_1} = \sqrt{2Y_k + 2\xi_1 X_k}. \quad (72)$$

A.2 Flow equations with $U(1)_A$ anomaly

In the case with $U(1)_A$ anomaly, the quantities $f_{k,i}$ in Eq. (55) read

$$\bar{v}_k = \frac{1}{2} k \left[24 \left(\frac{1}{E_{a_1}^2} + \frac{1}{E_\rho^2} \right) + \frac{6}{E_{a_0}^2} + \frac{2}{E_\eta^2} + \frac{2}{E_\sigma^2} + \frac{6}{E_\pi^2} \right], \quad (73)$$

$$\bar{w}_k = \frac{1}{2} k \left[\frac{32\bar{\xi}_1 \bar{W}_k'^2}{E_{a_0}^2 E_\sigma^4} + \frac{32\bar{\xi}_1 \bar{W}_k'^2}{E_{a_0}^4 E_\sigma^2} + \frac{192\bar{\xi}_1 \bar{Y}_k^2}{E_{a_1}^6} - \frac{24\bar{Y}_k}{E_{a_1}^4} - \frac{4(2\bar{\xi}_1 \bar{W}_k'' + \bar{W}_k')}{E_\sigma^4} - \frac{4(3\bar{W}_k' + \bar{X}_k)}{E_\pi^4} \right. \\ \left. + \frac{8\bar{\xi}_1 \bar{X}_k^2}{E_\pi^4 E_\eta^2} + \frac{8\bar{\xi}_1 \bar{X}_k^2}{E_\pi^2 E_\eta^4} - \frac{24\bar{Y}_k}{E_\rho^4} \right], \quad (74)$$

$$\bar{x}_k = \frac{1}{2} k \left\{ -\frac{32\bar{W}_k'^2}{E_{a_0}^2 E_\sigma^4} - \frac{32\bar{W}_k'^2}{E_{a_0}^4 E_\sigma^2} + \frac{24\bar{X}_k^2}{E_\pi^4 E_{a_0}^2} + \frac{24\bar{X}_k^2}{E_\pi^2 E_{a_0}^4} - \frac{24\bar{Y}_k}{E_{a_1}^4 \xi_1} - \frac{192\bar{Y}_k^2}{E_{a_1}^6} + \frac{4\bar{X}_k^2}{E_\eta^4 (-\bar{V}_k' + \bar{W}_k + \bar{\xi}_1 \bar{X}_k)} \right. \\ \left. - \frac{2\bar{X}_k^2}{E_\eta^2 (\bar{V}_k' - \bar{W}_k - \bar{\xi}_1 \bar{X}_k)^2} + \frac{4\bar{X}_k (\bar{W}_k - \bar{V}_k')}{E_\pi^2 E_\eta^2 \bar{\xi}_1 (-\bar{V}_k' + \bar{W}_k + \bar{\xi}_1 \bar{X}_k)} + \frac{2\bar{X}_k^2}{E_\pi^2 (\bar{V}_k' - \bar{W}_k - \bar{\xi}_1 \bar{X}_k)^2} \right. \\ \left. + \frac{4 \left[\bar{X}_k \left(\frac{1}{\xi_1} - \frac{\bar{X}_k}{-\bar{V}_k' + \bar{W}_k + \bar{\xi}_1 \bar{X}_k} \right) - 3\bar{X}_k' \right]}{E_\pi^4} + \frac{32(\bar{W}_k' + \bar{\xi}_1 \bar{X}_k' + \bar{X}_k)^2}{E_\eta^4 E_\sigma^2} + \frac{32(\bar{W}_k' + \bar{\xi}_1 \bar{X}_k' + \bar{X}_k)^2}{E_\eta^2 E_\sigma^4} \right. \\ \left. - \frac{4\bar{X}_k}{E_\pi^2 E_\eta^2 \bar{\xi}_1} - \frac{4 \left(2\bar{\xi}_1 \bar{X}_k'' + \frac{\bar{X}_k}{\xi_1} + 5\bar{X}_k' \right)}{E_\sigma^4} + \frac{24\bar{Y}_k}{\xi_1 E_\rho^4} \right\}, \quad (75)$$

$$\begin{aligned}
\bar{y}_k = \frac{1}{2}k \left\{ & -\frac{16\bar{q}^2\bar{Y}_k^2}{E_\pi^4 E_{a_1}^2 (\omega_n^2 + \bar{q}^2)} + \frac{32\bar{q}^2\bar{Y}_k^2}{E_{a_0}^4 E_{a_1}^2 (\omega_n^2 + \bar{q}^2)} - \frac{16\bar{q}^2\bar{Y}_k^2}{E_\pi^2 E_{a_1}^4 (\omega_n^2 + \bar{q}^2)} + \frac{32\bar{q}^2\bar{Y}_k^2}{E_{a_0}^2 E_{a_1}^4 (\omega_n^2 + \bar{q}^2)} \right. \\
& + \frac{32\bar{q}^2 (\bar{\xi}_1 \bar{Y}'_k + \bar{Y}_k + \bar{Z}'_k)^2}{E_{a_1}^4 E_\sigma^4 (\omega_n^2 + \bar{q}^2)} + \frac{32\bar{q}^2 (\bar{\xi}_1 \bar{Y}'_k + \bar{Y}_k + \bar{Z}'_k)^2}{E_{a_1}^4 E_\sigma^2 (\omega_n^2 + \bar{q}^2)} - \frac{16\bar{q}^2\bar{Y}_k^2}{E_{a_0}^4 (\omega_n^2 + \bar{q}^2) (\bar{\xi}_1 \bar{Y}_k + \bar{Z}_k)} \\
& + \frac{4\bar{Y}_k (5\bar{\xi}_1 \bar{Y}_k + \bar{Z}_k)}{E_{a_0}^4 \bar{\xi}_1 (\bar{\xi}_1 \bar{Y}_k + \bar{Z}_k)} + \frac{16\bar{q}^2\bar{Y}_k^2}{E_\pi^4 E_\rho^2 (\omega_n^2 + \bar{q}^2)} + \frac{16\bar{q}^2\bar{Y}_k^2}{E_\pi^2 E_\rho^4 (\omega_n^2 + \bar{q}^2)} \\
& - \frac{16\bar{q}^2 [\bar{Z}_k (\bar{\xi}_1 \bar{Y}'_k + \bar{Y}_k)^2 + 2\bar{Z}_k \bar{Z}'_k (\bar{\xi}_1 \bar{Y}'_k + \bar{Y}_k) - \bar{\xi}_1 \bar{Y}_k \bar{Z}'_k{}^2]}{E_\sigma^4 \bar{Z}_k (\omega_n^2 + \bar{q}^2) (\bar{\xi}_1 \bar{Y}_k + \bar{Z}_k)} - \frac{8\bar{\xi}_1 \bar{q}^2 \bar{Y}_k^3}{E_\pi^4 \bar{Z}_k (\omega_n^2 + \bar{q}^2) (\bar{\xi}_1 \bar{Y}_k + \bar{Z}_k)} \\
& - \frac{32\bar{q}^2 \bar{Z}'_k{}^2}{E_\rho^4 E_\sigma^2 (\omega_n^2 + \bar{q}^2)} - \frac{32\bar{q}^2 \bar{Z}'_k{}^2}{E_\rho^2 E_\sigma^4 (\omega_n^2 + \bar{q}^2)} - \frac{4\bar{Y}_k}{E_\eta^4 \bar{\xi}_1} + \frac{4 \left(\frac{\bar{Y}_k}{\bar{\xi}_1} + \frac{2\bar{\xi}_1 \bar{Y}_k^3}{\bar{\xi}_1 \bar{Y}_k \bar{Z}_k + \bar{Z}_k^2} - 3\bar{Y}'_k \right)}{E_\pi^4} \\
& \left. + \frac{4 \left[-2\bar{\xi}_1 \bar{Y}_k'' - \frac{\bar{Y}_k}{\bar{\xi}_1} + \frac{4\bar{Z}_k (\bar{\xi}_1 \bar{Y}'_k + \bar{Y}_k)^2 + 8\bar{Z}_k \bar{Z}'_k (\bar{\xi}_1 \bar{Y}'_k + \bar{Y}_k) - 4\bar{\xi}_1 \bar{Y}_k \bar{Z}'_k{}^2}{\bar{Z}_k (\bar{\xi}_1 \bar{Y}_k + \bar{Z}_k)} - 5\bar{Y}'_k \right]}{E_\sigma^4} \right\}, \tag{76}
\end{aligned}$$

$$\begin{aligned}
\bar{z}_k = \frac{1}{2}k \left\{ & \frac{16\bar{\xi}_1 \bar{q}^2 \bar{Y}_k^2}{E_\pi^4 E_{a_1}^2 (\omega_n^2 + \bar{q}^2)} + \frac{16\bar{\xi}_1 \bar{q}^2 \bar{Y}_k^2}{E_\pi^2 E_{a_1}^4 (\omega_n^2 + \bar{q}^2)} - \frac{8\bar{Y}_k}{E_{a_0}^4} - \frac{8\bar{\xi}_1 \bar{q}^2 \bar{Y}_k^2}{E_\pi^4 (\omega_n^2 + \bar{q}^2) (\bar{\xi}_1 \bar{Y}_k + \bar{Z}_k)} + \frac{32\bar{\xi}_1 \bar{q}^2 \bar{Z}'_k{}^2}{E_{a_0}^4 E_\sigma^2 (\omega_n^2 + \bar{q}^2)} \right. \\
& + \frac{32\bar{\xi}_1 \bar{q}^2 \bar{Z}'_k{}^2}{E_\rho^2 E_\sigma^4 (\omega_n^2 + \bar{q}^2)} - \frac{16\bar{\xi}_1 \bar{q}^2 \bar{Z}'_k{}^2}{E_\sigma^4 \bar{Z}_k (\omega_n^2 + \bar{q}^2)} + \frac{4 \left(-\frac{2\bar{Y}_k \bar{Z}_k}{\bar{\xi}_1 \bar{Y}_k + \bar{Z}_k} - 3\bar{Z}'_k \right)}{E_\pi^4} \\
& \left. - \frac{4 [\bar{Z}'_k (\bar{Z}_k - 4\bar{\xi}_1 \bar{Z}'_k) + 2\bar{\xi}_1 \bar{Z}_k \bar{Z}'_k{}^2]}{E_\sigma^4 \bar{Z}_k} \right\}, \tag{77}
\end{aligned}$$

with:

$$E_\sigma^2 = k^2 + \omega_n^2 + 2\bar{V}'_k + 4\bar{\xi}_1 \bar{V}_k'', \tag{78}$$

$$E_\pi^2 = k^2 + \omega_n^2 + 2\bar{V}'_k, \tag{79}$$

$$E_{a_0}^2 = k^2 + \omega_n^2 + 2\bar{W}_k, \tag{80}$$

$$E_\eta^2 = k^2 + \omega_n^2 + 2\bar{W}_k + 2\bar{\xi}_1 \bar{X}_k, \tag{81}$$

$$E_\rho^2 = k^2 + \omega_n^2 + 2\bar{Z}_k, \tag{82}$$

$$E_{a_1}^2 = k^2 + \omega_n^2 + 2\bar{Z}_k + 2\bar{\xi}_1 \bar{Y}_k. \tag{83}$$

In this case, the meson masses read:

$$m_\sigma = \sqrt{2\bar{V}'_k + 4\bar{\xi}_1 \bar{V}_k''}, \tag{84}$$

$$m_\pi = \sqrt{2\bar{V}'_k}, \tag{85}$$

$$m_{a_0} = \sqrt{2\bar{W}_k}, \tag{86}$$

$$m_\eta = \sqrt{2\bar{W}_k + 2\bar{\xi}_1 \bar{X}_k}, \tag{87}$$

$$m_\rho = \sqrt{2\bar{Z}_k}, \tag{88}$$

$$m_{a_1} = \sqrt{2\bar{Z}_k + 2\bar{\xi}_1 \bar{Y}_k}. \tag{89}$$

B Data interpolation

n data points y_j at sites x_j are approximated by a cubic spline f , such that the following expression is minimized:

$$p \sum_{j=1}^n w_j |y_j - f(x_j)|^2 + (1-p) \int \lambda(t) |D^2 f(t)|^2 dt . \quad (90)$$

The first term is an error measure, whereas the second a roughness measure. The default value for the weights w_j as well as for the weight function λ is one. The integration has to be performed over the smallest interval containing all data sites. p is a smoothing parameter. This method is used via the MATLAB `csaps` function.

For both fits in Fig. 1, all weights are equal to one and p is chosen to be 1×10^{-4} . In Fig. 2, we have $p = 1 \times 10^{-5}$ and $w_1 = 1 \times 10^4$ at $x_1 = 0$.

References

- [1] C. Vafa and E. Witten. Restrictions on symmetry breaking in vector-like gauge theories. *Nuclear Physics B*, 234(1):173–188, 1984.
- [2] Y. Nambu and G. Jona-Lasinio. Dynamical model of elementary particles based on an analogy with superconductivity. I. *Phys. Rev.*, 122:345–358, 1961.
- [3] Y. Nambu and G. Jona-Lasinio. Dynamical model of elementary particles based on an analogy with superconductivity. II. *Phys. Rev.*, 124:246–254, 1961.
- [4] A. Butti, A. Pelissetto, and E. Vicari. On the nature of the finite-temperature transition in QCD. *Journal of High Energy Physics*, 2003(08):029, 2003.
- [5] P. Braun-Munzinger, K. Redlich, and J. Stachel. Particle production in heavy ion collisions. arXiv:nucl-th/0304013v1, 2003.
- [6] R. D. Pisarski. Applications of chiral symmetry. arXiv:hep-ph/9503330v1, 1995.
- [7] G. E. Brown and M. Rho. Scaling effective Lagrangians in a dense medium. *Phys. Rev. Lett.*, 66:2720–2723, 1991.
- [8] M. Harada and C. Sasaki. Dropping ρ and A_1 meson masses at the chiral phase transition in the generalized hidden local symmetry. *Phys. Rev. D*, 73:036001, 2006.
- [9] B. Friman et al. *The CBM Physics Book: Compressed Baryonic Matter in Laboratory Experiments*. Springer, 2011.
- [10] R. Rapp and J. Wambach. Chiral symmetry restoration and dileptons in relativistic heavy-ion collisions. In *Advances in Nuclear Physics*, volume 25, pages 1–205. Springer US, 2002.
- [11] G. Agakichiev et al. e^+e^- -pair production in Pb-Au collisions at 158 GeV per nucleon. *Eur. Phys. J. C - Particles and Fields*, 41(4):475–513, 2005.
- [12] S. Damjanovic. NA60 results on the ρ spectral function in In-In collisions. *Nuclear Physics A*, 783(1-4):327–334, 2007.
- [13] R. Vértési, T. Csörgő, and J. Sziklai. Significant in-medium η' mass reduction in $\sqrt{s_{NN}}=200$ GeV Au+Au collisions at the BNL relativistic heavy ion collider. *Phys. Rev. C*, 83:054903, 2011.
- [14] J. Kapusta, D. Kharzeev, and L. McLerran. Return of the prodigal Goldstone boson. *Phys. Rev. D*, 53:5028–5033, 1996.
- [15] K. Fukushima and T. Hatsuda. The phase diagram of dense QCD. *Reports on Progress in Physics*, 74(1):014001, 2011.
- [16] D. J. Gross, R. D. Pisarski, and L. G. Yaffe. QCD and instantons at finite temperature. *Rev. Mod. Phys.*, 53:43–80, 1981.
- [17] R. D. Pisarski and F. Wilczek. Remarks on the chiral phase transition in chromodynamics. *Phys. Rev. D*, 29:338–341, 1984.
- [18] M. Grahl and D. H. Rischke. Functional renormalization group study of the two-flavor linear sigma model in the presence of the axial anomaly. *Phys. Rev. D*, 88:056014, 2013.
- [19] A. Pelissetto and E. Vicari. Relevance of the axial anomaly at the finite-temperature chiral transition in QCD. *Phys. Rev. D*, 88:105018, 2013.

- [20] M. Grahl. $U(2)_A \times U(2)_V$ -symmetric fixed point from the functional renormalization group. *Phys. Rev. D*, 90:117904, 2014.
- [21] C. Bernard et al. (MILC Collaboration). QCD thermodynamics with three flavors of improved staggered quarks. *Phys. Rev. D*, 71:034504, 2005.
- [22] M. Cheng et al. Transition temperature in QCD. *Phys. Rev. D*, 74:054507, 2006.
- [23] Y. Aoki, Z. Fodor, S.D. Katz, and K.K. Szabo. The QCD transition temperature: Results with physical masses in the continuum limit. *Physics Letters B*, 643(1):46 – 54, 2006.
- [24] Y. Maezawa et al. Thermodynamics of two-flavor lattice QCD with an improved Wilson quark action at non-zero temperature and density. *J. Phys. G: Nucl. Part. Phys.*, 34:S651–654, 2007.
- [25] M. Cheng et al. QCD equation of state with almost physical quark masses. *Phys. Rev. D*, 77:014511, 2008.
- [26] Y. Aoki et al. The QCD transition temperature: results with physical masses in the continuum limit II. *Journal of High Energy Physics*, 2009(06):088, 2009.
- [27] A. Bazavov et al. Equation of state and QCD transition at finite temperature. *Phys. Rev. D*, 80:014504, 2009.
- [28] M. Cheng et al. Finite temperature QCD using $2 + 1$ flavors of domain wall fermions at $N_t = 8$. *Phys. Rev. D*, 81:054510, 2010.
- [29] V. G. Bornyakov et al. (QCDSF-DIK Collaboration). Probing the finite temperature phase transition with $N_f = 2$ nonperturbatively improved Wilson fermions. *Phys. Rev. D*, 82:014504, 2010.
- [30] A. Bazavov and P. Petreczky. Deconfinement and chiral transition with the highly improved staggered quark (HISQ) action. *J.Phys.Conf.Ser.*, 230:012014, 2010.
- [31] S. Borsanyi et al. Is there still any T_c mystery in lattice QCD? Results with physical masses in the continuum limit III. *JHEP*, 1009:073, 2010.
- [32] A. Bazavov et al. Chiral and deconfinement aspects of the QCD transition. *Phys. Rev. D*, 85:054503, 2012.
- [33] G. Endrödi. QCD phase diagram: overview of recent lattice results. *Journal of Physics: Conference Series*, 503(1):012009, 2014.
- [34] S. Aoki, H. Fukaya, and Y. Taniguchi. Chiral symmetry restoration, the eigenvalue density of the Dirac operator, and the axial $U(1)$ anomaly at finite temperature. *Phys. Rev. D*, 86:114512, 2012.
- [35] G. Cossu et al. Finite temperature study of the axial $U(1)$ symmetry on the lattice with overlap fermion formulation. *Phys. Rev. D*, 87:114514, 2013.
- [36] S. Sharma, V. Dick, F. Karsch, E. Laermann, and S. Mukherjee. Investigation of the $U_A(1)$ in high temperature QCD on the lattice. *PoS, LATTICE2013:164*, 2014.
- [37] T. Bhattacharya et al. (HotQCD Collaboration). QCD phase transition with chiral quarks and physical quark masses. *Phys. Rev. Lett.*, 113:082001, 2014.
- [38] Viktor Dick, Frithjof Karsch, Edwin Laermann, Swagato Mukherjee, and Sayantan Sharma. Microscopic origin of $U_A(1)$ symmetry violation in the high temperature phase of QCD. *Phys. Rev.*, D91(9):094504, 2015.
- [39] C. Wetterich. Exact evolution equation for the effective potential. *Physics Letters B*, 301(1):90 – 94, 1993.
- [40] T. R. Morris. The exact renormalization group and approximate solutions. *International Journal of Modern Physics A*, 09(14):2411–2449, 1994.
- [41] J. M. Pawłowski. Aspects of the functional renormalisation group. *Annals of Physics*, 322(12):2831 – 2915, 2007.
- [42] P. Kopietz, L. Bartosch, and F. Schütz. *Introduction to the Functional Renormalization Group*. Springer, 2010.
- [43] J. Berges, N. Tetradis, and C. Wetterich. Non-perturbative renormalization flow in quantum field theory and statistical physics. *Physics Reports*, 363(4-6):223 – 386, 2002.
- [44] D.-U. Jungnickel and C. Wetterich. Effective action for the chiral quark-meson model. *Phys. Rev. D*, 53:5142–5175, 1996.
- [45] B.-J. Schaefer and J. Wambach. Renormalization group approach towards the QCD phase diagram. *Physics of Particles and Nuclei*, 39(7):1025–1032, 2008.
- [46] J. Berges, D. U. Jungnickel, and C. Wetterich. Two flavor chiral phase transition from nonperturbative flow equations. *Phys. Rev.*, D59:034010, 1999.

- [47] B.-J. Schaefer and J. Wambach. The phase diagram of the quark-meson model. *Nuclear Physics A*, 757(3-4):479 – 492, 2005.
- [48] B.-J. Schaefer and J. Wambach. Susceptibilities near the QCD (tri)critical point. *Phys. Rev. D*, 75:085015, 2007.
- [49] B. J. Schaefer, J. M. Pawłowski, and J. Wambach. Phase structure of the Polyakov-quark-meson model. *Phys. Rev. D*, 76:074023, 2007.
- [50] Tina Katharina Herbst, Jan M. Pawłowski, and Bernd-Jochen Schaefer. The phase structure of the Polyakov–quark-meson model beyond mean field. *Phys. Lett.*, B696:58–67, 2011.
- [51] V. Skokov, B. Stokic, B. Friman, and K. Redlich. Meson fluctuations and thermodynamics of the Polyakov loop extended quark-meson model. *Phys. Rev.*, C82:015206, 2010.
- [52] Jens Braun, Holger Gies, and Jan M. Pawłowski. Quark Confinement from Color Confinement. *Phys. Lett.*, B684:262–267, 2010.
- [53] Nils Strodthoff, Bernd-Jochen Schaefer, and Lorenz von Smekal. Quark-meson-diquark model for two-color QCD. *Phys. Rev.*, D85:074007, 2012.
- [54] Tina K. Herbst, Jan M. Pawłowski, and Bernd-Jochen Schaefer. Phase structure and thermodynamics of QCD. *Phys. Rev.*, D88(1):014007, 2013.
- [55] Tina Katharina Herbst, Mario Mitter, Jan M. Pawłowski, Bernd-Jochen Schaefer, and Rainer Stiele. Thermodynamics of QCD at vanishing density. *Phys. Lett.*, B731:248–256, 2014.
- [56] Ralf-Arno Tripolt, Nils Strodthoff, Lorenz von Smekal, and Jochen Wambach. Spectral Functions for the Quark-Meson Model Phase Diagram from the Functional Renormalization Group. *Phys. Rev.*, D89(3):034010, 2014.
- [57] Nils Strodthoff and Lorenz von Smekal. Polyakov-Quark-Meson-Diquark Model for two-color QCD. *Phys. Lett.*, B731:350–357, 2014.
- [58] J. M. Pawłowski. Exact flow equations and the U(1) problem. *Phys. Rev.*, D58:045011, 1998.
- [59] Bernd-Jochen Schaefer and Mario Mitter. Three-flavor chiral phase transition and axial symmetry breaking with the functional renormalization group. *Acta Phys. Polon. Supp.*, 7(1):81–90, 2014.
- [60] M. Mitter and B.-J. Schaefer. Fluctuations and the axial anomaly with three quark flavors. *Phys. Rev. D*, 89:054027, 2014.
- [61] Jens O. Andersen, William R. Naylor, and Anders Tranberg. Chiral and deconfinement transitions in a magnetic background using the functional renormalization group with the Polyakov loop. *JHEP*, 04:187, 2014.
- [62] K. Kamikado and T. Kanazawa. Chiral dynamics in a magnetic field from the functional renormalization group. *Journal of High Energy Physics*, 2014(3), 2014.
- [63] K. Fukushima, K. Kamikado, and B. Klein. Second-order and fluctuation-induced first-order phase transitions with functional renormalization group equations. *Phys. Rev. D*, 83:116005, 2011.
- [64] G. Fejős. Fluctuation induced first order phase transition in $U(n) \times U(n)$ models using chiral invariant expansion of functional renormalization group flows. *Phys. Rev. D*, 90:096011, 2014.
- [65] J. Braun, A. Eichhorn, H. Gies, and J. M. Pawłowski. On the nature of the phase transition in SU(N), Sp(2) and E(7) Yang-Mills theory. *Eur. Phys. J. C*, 70(3):689 – 702, 2010.
- [66] J. Braun, L. M. Haas, F. Marhauser, and J. M. Pawłowski. Phase structure of two-flavor QCD at finite chemical potential. *Phys. Rev. Lett.*, 106:022002, 2011.
- [67] L. Fister and J. M. Pawłowski. Confinement from correlation functions. *Phys. Rev. D*, 88:045010, 2013.
- [68] J. Braun, L. Fister, J. M. Pawłowski, and F. Rennecke. From quarks and gluons to hadrons: chiral symmetry breaking in dynamical QCD. arXiv:1412.1045 [hep-ph], 2014.
- [69] Mario Mitter, Jan M. Pawłowski, and Nils Strodthoff. Chiral symmetry breaking in continuum QCD. *Phys. Rev.*, D91:054035, 2015.
- [70] M. Drews, T. Hell, B. Klein, and W. Weise. Thermodynamic phases and mesonic fluctuations in a chiral nucleon-meson model. *Phys. Rev. D*, 88:096011, 2013.
- [71] M. Drews, T. Hell, B. Klein, and W. Weise. Dense nucleonic matter and the renormalization group. *EPJ Web of Conferences*, 66:04008, 2014.
- [72] M. Drews and W. Weise. Functional renormalization group approach to neutron matter. *Physics Letters B*, 738(0):187 – 190, 2014.

- [73] M. Drews and W. Weise. Functional renormalization group study of nuclear and neutron matter. arXiv:1410.8707 [nucl-th], 2014.
- [74] M. Drews and W. Weise. From asymmetric nuclear matter to neutron stars: A functional renormalization group study. *Phys. Rev. C*, 91:035802, 2015.
- [75] F. Rennecke. The vacuum structure of vector mesons in QCD. arXiv:1504.03585 [hep-ph], 2015.
- [76] D. Parganlija, F. Giacosa, and D. H. Rischke. Vacuum properties of mesons in a linear sigma model with vector mesons and global chiral invariance. *Phys. Rev. D*, 82:054024, 2010.
- [77] D. Parganlija. Quarkonium phenomenology in vacuum. arXiv:1208.0204v1 [hep-ph], 2012.
- [78] D. Parganlija, P. Kovács, Gy. Wolf, F. Giacosa, and D. H. Rischke. Meson vacuum phenomenology in a three-flavor linear sigma model with (axial-)vector mesons. *Phys. Rev. D*, 87:014011, 2013.
- [79] Florian Divotgey, Francesco Giacosa, and Dirk H. Rischke. In preparation.
- [80] J. J. Sakurai. Theory of strong interactions. *Annals of Physics*, 11(1):1 – 48, 1960.
- [81] S. Strüber and D. H. Rischke. Vector and axial-vector mesons at nonzero temperature within a gauged linear sigma model. *Phys. Rev. D*, 77:085004, 2008.
- [82] J. Schwinger. A theory of the fundamental interactions. *Annals of Physics*, 2(5):407 – 434, 1957.
- [83] M. Gell-Mann and M. Levy. The axial vector current in beta decay. *Il Nuovo Cimento*, 16(4):705–726, 1960.
- [84] S. Gasiorowicz and D. A. Geffen. Effective Lagrangians and field algebras with chiral symmetry. *Rev. Mod. Phys.*, 41:531–573, 1969.
- [85] J. Boguta. A saturating chiral field theory of nuclear matter. *Physics Letters B*, 120(1–3):34 – 38, 1983.
- [86] P. Ko and S. Rudaz. Phenomenology of scalar and vector mesons in the linear σ model. *Phys. Rev. D*, 50:6877–6894, 1994.
- [87] M. Urban, M. Buballa, and J. Wambach. Vector and axial-vector correlators in a chirally symmetric model. *Nuclear Physics A*, 697(1-2):338 – 371, 2002.
- [88] K. Kawarabayashi and M. Suzuki. Partially conserved axial-vector current and the decays of vector mesons. *Phys. Rev. Lett.*, 16:255–257, 1966.
- [89] Riazuddin and Fayyazuddin. Algebra of current components and decay widths of ρ and K^* mesons. *Phys. Rev.*, 147:1071–1073, 1966.
- [90] K. A. Olive et al. (Particle Data Group). The review of particle physics. *Chinese Physics C*, 38:090001, 2014.
- [91] K. G. Wilson. Non-Lagrangian models of current algebra. *Phys. Rev.*, 179:1499–1512, 1969.
- [92] K. G. Wilson. Renormalization group and critical phenomena. I. Renormalization group and the Kadanoff scaling picture. *Phys. Rev. B*, 4:3174–3183, 1971.
- [93] K. G. Wilson. Renormalization group and critical phenomena. II. Phase-space cell analysis of critical behavior. *Phys. Rev. B*, 4:3184–3205, 1971.
- [94] K. G. Wilson and M. E. Fisher. Critical exponents in 3.99 dimensions. *Phys. Rev. Lett.*, 28:240–243, 1972.
- [95] K. G. Wilson. Feynman-graph expansion for critical exponents. *Phys. Rev. Lett.*, 28:548–551, 1972.
- [96] K. G. Wilson and J. Kogut. The renormalization group and the ϵ expansion. *Physics Reports*, 12(2):75 – 199, 1974.
- [97] K. G. Wilson. The renormalization group: Critical phenomena and the Kondo problem. *Rev. Mod. Phys.*, 47:773–840, 1975.
- [98] D. H. Rischke and W. Greiner. A functional integral approach to the thermodynamics of the σ - ω model. *International Journal of Modern Physics E*, 03(04):1157–1194, 1994.
- [99] C. Itzykson and J. B. Zuber. *Quantum Field Theory*. McGraw-Hill, 1985.
- [100] H. Ruegg and M. Ruiz-Altaba. The Stueckelberg field. *International Journal of Modern Physics A*, 19(20):3265–3347, 2004.
- [101] D. F. Litim. Optimized renormalization group flows. *Phys. Rev. D*, 64:105007, 2001.
- [102] D. F. Litim and J. M. Pawłowski. Non-perturbative thermal flows and resummations. *Journal of High Energy Physics*, 2006(11):026, 2006.

- [103] J.-P. Blaizot, A. Ipp, R. Mendez-Galain, and N. Wschebor. Perturbation theory and non-perturbative renormalization flow in scalar field theory at finite temperature. *Nuclear Physics A*, 784(1-4):376 – 406, 2007.
- [104] A. Patkos. Invariant formulation of the functional renormalization group method for $U(n)\times U(n)$ symmetric matrix models. *Modern Physics Letters A*, 27(36):1250212, 2012.
- [105] F. R. Brown et al. On the existence of a phase transition for QCD with three light quarks. *Phys. Rev. Lett.*, 65:2491–2494, 1990.
- [106] O. Philipsen. Status of lattice studies of the QCD phase diagram. *Progress of Theoretical Physics Supplement*, 174:206–213, 2008.
- [107] A. Nieto. Evaluating sums over the Matsubara frequencies. *Computer Physics Communications*, 92(1):54 – 64, 1995.
- [108] Z. Fodor and S. D. Katz. Critical point of QCD at finite T and μ , lattice results for physical quark masses. *Journal of High Energy Physics*, 2004(04):050, 2004.
- [109] Robert L. Jaffe. Multi-Quark Hadrons. 1. The Phenomenology of (2 Quark 2 anti-Quark) Mesons. *Phys. Rev.*, D15:267, 1977.
- [110] Achim Heinz, Stefan Struber, Francesco Giacosa, and Dirk H. Rischke. Role of the tetraquark in the chiral phase transition. *Phys. Rev.*, D79:037502, 2009.
- [111] C. DeTar and T. Kunihiro. Linear sigma model with parity doubling. *Phys. Rev. D*, 39:2805–2808, 1989.
- [112] S. Wilms, F. Giacosa, and D. H. Rischke. Pion-nucleon scattering within a gauged linear sigma model with parity-doubled nucleons. *Int.J.Mod.Phys.*, E16:2388–2393, 2007.
- [113] L. Y. Glozman. Alternative experimental evidence for chiral restoration in excited baryons. *Phys. Rev. Lett.*, 99:191602, 2007.
- [114] D. Jido, T. Hatsuda, and T. Kunihiro. Chiral-symmetry realization for even- and odd-parity baryon resonances. *Phys. Rev. Lett.*, 84:3252–3255, 2000.